DEVELOPMENT OF A BIASING SCHEME TO IMPROVE INITIAL DYNAMICAL MODEL FORECASTS OF TROPICAL CYCLONE MOTION.

John David Shewchuk

NAVAL POSTGRADUATE SCHOOL
Monterey, California

THESIS

DEVELOPMENT OF A BIASING SCHEME
TO IMPROVE INITIAL DYNAMICAL MODEL FORECASTS
OF TROPICAL CYCLONE MOTION

by

John David Shewchuk

June 1977

Thesis Advisor: R. L. Elsberry

Approved for public release; distribution unlimited.

SECURITY CLASSIFICATION OF THIS PAGE (When Data Entered)

REPORT DOCUMENTATION PAGE

READ INSTRUCTIONS BEFORE COMPLETING FORM

1. REPORT NUMBER	2. GOVT ACCESSION NO. / 3. RECIPIENT'S CATALOG NUMBER
4. TITLE (and Subtitle): Development of a Biasing Scheme to Improve Initial Dynamical Model Forecasts of Tropical Cyclone Motion	5. TYPE OF REPORT & PERIOD COVERED: Master's Thesis; June 1977
	6. PERFORMING ORG. REPORT NUMBER
7. AUTHOR(s): John David Shewchuk	8. CONTRACT OR GRANT NUMBER(s)
9. PERFORMING ORGANIZATION NAME AND ADDRESS: Naval Postgraduate School, Monterey, California 93940	10. PROGRAM ELEMENT, PROJECT, TASK AREA & WORK UNIT NUMBERS
11. CONTROLLING OFFICE NAME AND ADDRESS: Naval Postgraduate School, Monterey, California 93940	12. REPORT DATE: June 1977
	13. NUMBER OF PAGES: 93
14. MONITORING AGENCY NAME & ADDRESS (if different from Controlling Office): Naval Postgraduate School, Monterey, California 93940	15. SECURITY CLASS. (of this report): Unclassified
	15a. DECLASSIFICATION/DOWNGRADING SCHEDULE

16. DISTRIBUTION STATEMENT (of this Report)

Approved for public release; distribution unlimited.

17. DISTRIBUTION STATEMENT (of the abstract entered in Block 20, if different from Report)

18. SUPPLEMENTARY NOTES

19. KEY WORDS (Continue on reverse side if necessary and identify by block number)

20. ABSTRACT (Continue on reverse side if necessary and identify by block number)

A technique of adjusting the initial steering currents to improve the short-term forecasts of tropical cyclone motion with a dynamical model was tested. Initial tests were performed with hand-analyzed data, although 41 objectively-analyzed cases were also examined to evaluate operational feasibility. Several schemes to track the storm objectively resulted in the use of the streamfunction minimum to define the storm centers.

DD FORM 1 JAN 73 1473 EDITION OF 1 NOV 65 IS OBSOLETE
S/N 0102-014-6601

SECURITY CLASSIFICATION OF THIS PAGE (When Data Entered)

Two biasing approaches were developed. The first used statistical regression equations to predict the initial storm motion, while the second used an empirical relationship to define the initial steering current. Various areal distributions of the bias corrections were then applied to the initial wind fields. Results from these tests indicated improved forecast accuracy if the largest corrections were applied at some distance from the storm center. The biasing decreased average forecast errors for the first 30 hours by about 40% for the hand-analyzed cases and about 30% for the objectively-analyzed cases, with 25% and 15% decreases after 48 hours, respectively. Significant improvements were also observed in the standard deviation of track errors, with averaged decreases of 60% for hand-analyzed cases and 45% for objectively-analyzed cases.

Approved for public release; distribution unlimited.

Development of a Biasing Scheme to Improve Initial Dynamical Model Forecasts of Tropical Cyclone Motion

by

John David Shewchuk
Captain, United States Air Force
B.S., The Pennsylvania State University, 1972

Submitted in partial fulfillment of the
requirements for the degree of

MASTER OF SCIENCE IN METEOROLOGY

from the

NAVAL POSTGRADUATE SCHOOL
June 1977

ABSTRACT

A technique of adjusting the initial steering currents to improve the short-term forecasts of tropical cyclone motion with a dynamical model was tested. Initial tests were performed with hand-analyzed data, although 41 objectively-analyzed cases were also examined to evaluate operational feasibility. Several schemes to track the storm objectively resulted in the use of the streamfunction minimum to define the storm centers.

Two biasing approaches were developed. The first used statistical regression equations to predict the initial storm motion, while the second used an empirical relationship to define the initial steering current. Various areal distributions of the bias corrections were then applied to the initial wind fields. Results from these tests indicated improved forecast accuracy if the largest corrections were applied at some distance from the storm center. The biasing decreased average forecast errors for the first 30 hours by about 40% for the hand-analyzed cases and about 30% for the objectively-analyzed cases, with 25% and 15% decreases after 48 hours, respectively. Significant improvements were also observed in the standard deviation of track errors, with averaged decreases of 60% for hand-analyzed cases and 45% for objectively-analyzed cases.

TABLE OF CONTENTS

LIST OF TABLES

LIST OF FIGURES

LIST OF SYMBOLS

t	Time variable
u	Velocity component in the x-direction
v	Velocity component in the y-direction
x, y	West-east, north-south space axes
θ	Potential temperature
f	Coriolis parameter
τ_{xx}, τ_{yx}	Components of shear stress per unit area by u wind component
τ_{xy}, τ_{yy}	Components of shear stress per unit area by v wind component
g	Acceleration of gravity
M	Map factor
z	Vertical distance above 1000 millibar surface
ϕ	Geopotential height
ϕ_{1000}	Geopotential height of 1000 millibar surface
ω	Vertical velocity in pressure coordinates
P	Pressure (space axis in vertical)
ψ	Streamfunction
ζ	Vorticity
C_p	Specific heat at constant pressure
Δ	Finite difference operator
R	Gas constant for dry air
ρ	Atmospheric density
$\overline{S}$	Average of S over the entire grid

$\tilde{S}$	Average of S along one row of the grid
u'	Perturbation component in the x-direction
∇^2	Laplacian operator
U_M	Predicted model component in the x-direction
V_M	Predicted model component in the y-direction
Δu	Unit bias corrector in the x-direction
Δv	Unit bias corrector in the y-direction
$\overline{U}$	Vertically averaged steering mean current component in the x-direction
$\overline{V}$	Vertically averaged steering mean current component in the y-direction

ACKNOWLEDGEMENTS

The author wishes especially to thank Professor R. L. Elsberry for his patience and guidance throughout the course of this research.

Special appreciation is extended to Lt. D. E. Hinsman, USN, whose concerned interest and continual assistance enabled the majority of the tests and results presented herein possible.

The author also wishes to thank Professors G. J. Haltiner and C. P. Chang for reviewing the manuscript and making several useful suggestions.

The personalized service received from the W. R. Church Computer Center night shift personnel gave invaluable numerical support. Lts. (USN) W. F. Johnson and O. M. Lubeck extended expert computer assistance in the solution of several technical difficulties.

An affectionate thank you is extended to the author's wife, Judy, for her devoted patience during the research and unyielding assistance with preliminary typing of the manuscript.

I. INTRODUCTION

Prediction of tropical storms is a major concern worldwide. The need to know storm conditions in advance has produced a variety of prediction methods. Subjective methods, including persistence, have normally produced good short-range forecasts. The occurrence of storm recurvature is an especially difficult problem for any prognostic scheme, whether subjective or objective. This was a significant problem encountered during the 1975 western Pacific typhoon season. An unusually large number of the storms tracked north, while some quickly recurved. As a result, all error statistics were higher than normal. Meanwhile, much progress has been made in the numerical simulation of characteristics of tropical storms, such as intensity and even spiral bands (Anthes et al, 1974), but the major emphasis has focused on forecasting storm movement (Hovermale et al, 1976, and Ley, 1975). A prime objective of the latest multi-level, nested-grid models has been to improve medium- and long-range motion forecasts over those of persistence, analog, or statistical forecast techniques. Yet, no matter how sophisticated the numerical models may be, initialization with limited and poor data may produce undesirable consequences. Even if the analysis is good, the model should at least be able to simulate the initial storm motion with reasonable accuracy. It

is observed that dynamical models occasionally produce irregular storm tracks, and the forecast motion is generally too slow. A model cannot be expected to operate at its full potential and produce extended, accurate forecasts if the short-term forecast is bad. Specification of the initial data fields seems to be a likely source of error in these situations.

Since the resources required to increase the amount of high quality data are costly and will require considerable amounts of time to acquire, alternative methods for improving initialization of models should be considered. Of the resources currently available, the valuable information represented by the recent movement of the tropical storm has yet to be effectively utilized in a dynamical model. All statistical schemes for predicting tropical storm motion (Renard et al, 1972) rely heavily on the current movement of the storm. Perhaps the most direct approach for improving a tropical cyclone model is to correct, or bias, the initial wind fields to reflect the recently observed motion of the storm. It is therefore the primary objective of this thesis to develop and evaluate a method of biasing the initial data to improve the tropical cyclone model forecasts.

The primitive-equation, three-layer, tropical cyclone model (TCM) developed by Elsberry and Harrison (1971) and Harrison (1973) was used with a uniform coarse grid. Although this model is capable of triply-nested operation (Harrison, 1973), results from Ley and Elsberry (1976) show that the

coarse and nested grids produced nearly identical results in a selected case study based on hand-analyzed data. Because of the new biasing scheme tested, the simpler, uniform grid model allowed for easier modifications and less computer requirements.

A bias corrector is desired that would adjust the initial data fields initially to steer the storm according to its recent movement. If one could estimate the initial storm displacement as part of the diagnostic phase of the model, a comparison could then be made with the actual storm movement. If, upon comparison, the storm's predicted initial motion deviated significantly from the recently observed motion, a bias could be applied to correct the initial model-predicted storm track and the subsequent forecasts. In this research, the initial model storm movement is calculated from a statistical regression equation, and the bias is applied to the initial wind fields. To accomplish this, a steering current relating the storm movement to the surrounding wind fields was first defined. Then, based on prior storm track information, a regression equation was developed to predict the storm movement from the steering currents in the three-layer model. After comparison of the observed and predicted storm motion and determination of the required bias, some experimentation was necessary to derive the form of the bias to be applied to the original data fields. In this way, the adjusted steering current could steer the storm in the desired direction.

The biasing method developed was tested on 48 cases in the western Pacific region, most of which were of typhoon intensity. Seven cases (two storms) used hand-analyzed data supplied by the Joint Typhoon Warning Center (JTWC), Guam, while the other 41 cases (13 storms) were based on operationally-analyzed data obtained from the Fleet Numerical Weather Central (FNWC), Monterey, California. Since the hand-analzyed cases provided more accurate initial wind fields as compared to FNWC's objective analyses (Elsberry, 1977), they were used for the majority of the tests of the biasing method. The contrasting tracks of these two 1974 storms (one moved westward while the other recurved) also provided the directional diversity needed to develop a flexible biasing scheme. But the most important result required of this scheme was the need to improve consistently the TCM's initial forecasts. Upon completion of the testing of the various biasing techniques using the hand-analyzed cases, further tests with the operationally-analyzed cases from 1975 were evaluated for operational feasibility. All forecast positions, biased and unbiased, were verified against the best tracks from the Annual Typhoon Reports (1974, 1975) published by JTWC.

Two approaches for biasing the initial data to improve the steering current were used. The first approach, which was previously described, compared an observed with a predicted storm track to determine the required bias. The second approach incorporated an empirical relation between

the storm motion and the steering current based on the results by George and Gray (1976). As a result of these relationships, the empirical steering current was known, and could be compared to the observed current to produce a bias corrector. The methods and results from these two approaches are presented for comparison.

II. THE TROPICAL CYCLONE MODEL

A. THE MODEL

The Tropical Cyclone Model (TCM) characteristics are presented in the Appendix. A more complete discussion may be found in Ley (1975). The TCM is a three-layer, primitive equation model in pressure coordinates. It is a channeled model with free slip conditions on the north and south walls and cyclic conditions on the east and west boundaries.

B. MODEL MODIFICATIONS

Since this model was primarily developed for movement forecasts, a crude, five-grid point, heating function was centered over the storm to counteract the dispersion of the vortex due to the finite differencing (Ley and Elsberry, 1976). Because the heating pattern was centered on the grid point nearest the pressure minimum, it was sometimes applied to the rear quadrants of the storm's direction. Consequently, the track of the center tended to zigzag or oscillate. A comparison of the 48-hour tracks of one of the storms with and without heating (both without friction) is given in Fig. 1. In almost all cases, this heating caused a retardation of storm speed and directional backing with respect to the non-heated cases. Therefore, all subsequent case studies were computed without the effects of heating or friction.

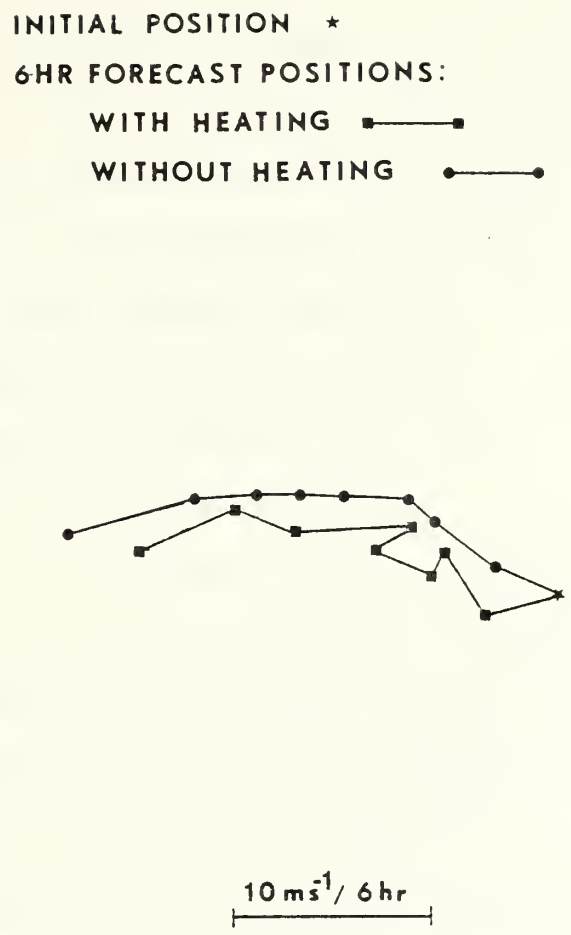

Fig. 1. Comparison of forecast tracks with and without vortex heating starting from 00 GMT on 25 Nov. 1974.

C. THE TRACKING METHOD

An objective method of tracking the storm's movement was needed for consistent comparisons. A tracking algorithm, developed by Lt. D. Hinsman, USN, at FNWC, interpolates the maximum and minimum values of any data field. Sequences of six-hourly, model-predicted vorticity, geopotential and streamfunction fields defined by

$$\text{850 mb, Vorticity } (\zeta) = \partial v/\partial x - \partial u/\partial y \qquad (1)$$

$$\text{1000 mb, Geopotential } (\phi) = gz \qquad (2)$$

$$\text{850 mb, Streamfunction } (\psi),$$

$$\text{where } \nabla^2\psi = \zeta = \partial v/\partial x - \partial u'/\partial y \qquad (3)$$

were used to estimate the storm center movement (Fig. 2). Fig. 3 compares the 48-hour center forecasts by the three methods tested. The initial storm center was located accurately in all fields, since the storm was initially bogused symmetrically (reference Numerical Environment Products Manual, 1975).

Each method of storm-center tracking was subjectively evaluated. After an approximately 18-hour forecast period, significant asymmetrical troughing sometimes appeared in the wind fields. Since the coarse-mesh grid was unable to resolve the storm's radius of maximum winds, these inner winds may become quite weak. The shear and curvature contributions to the vorticity were much greater in the induced wind troughs. As a result, the vorticity centers may become greater in the trough as far as 600 km from the storm's wind circulation center. Hovermale et al (1976) experienced this tracking problem even in a model with 60-km grid spacing.

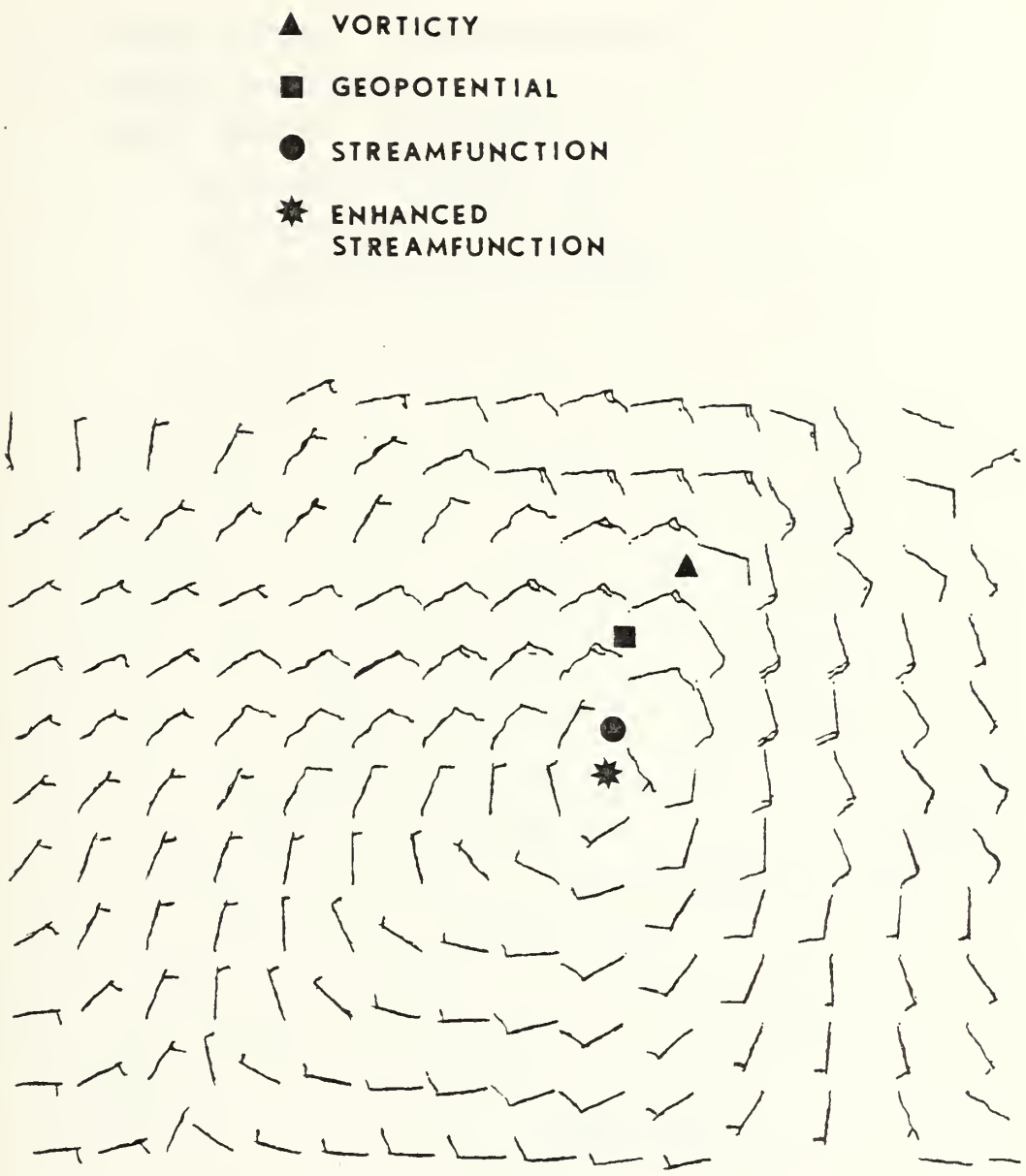

Fig. 2. Predicted 850-mb wind field at 30 h starting from 00 GMT 27 Nov. 1974 with vortex center determination from vorticity, geopotential, streamfunction and enhanced streamfunction fields.

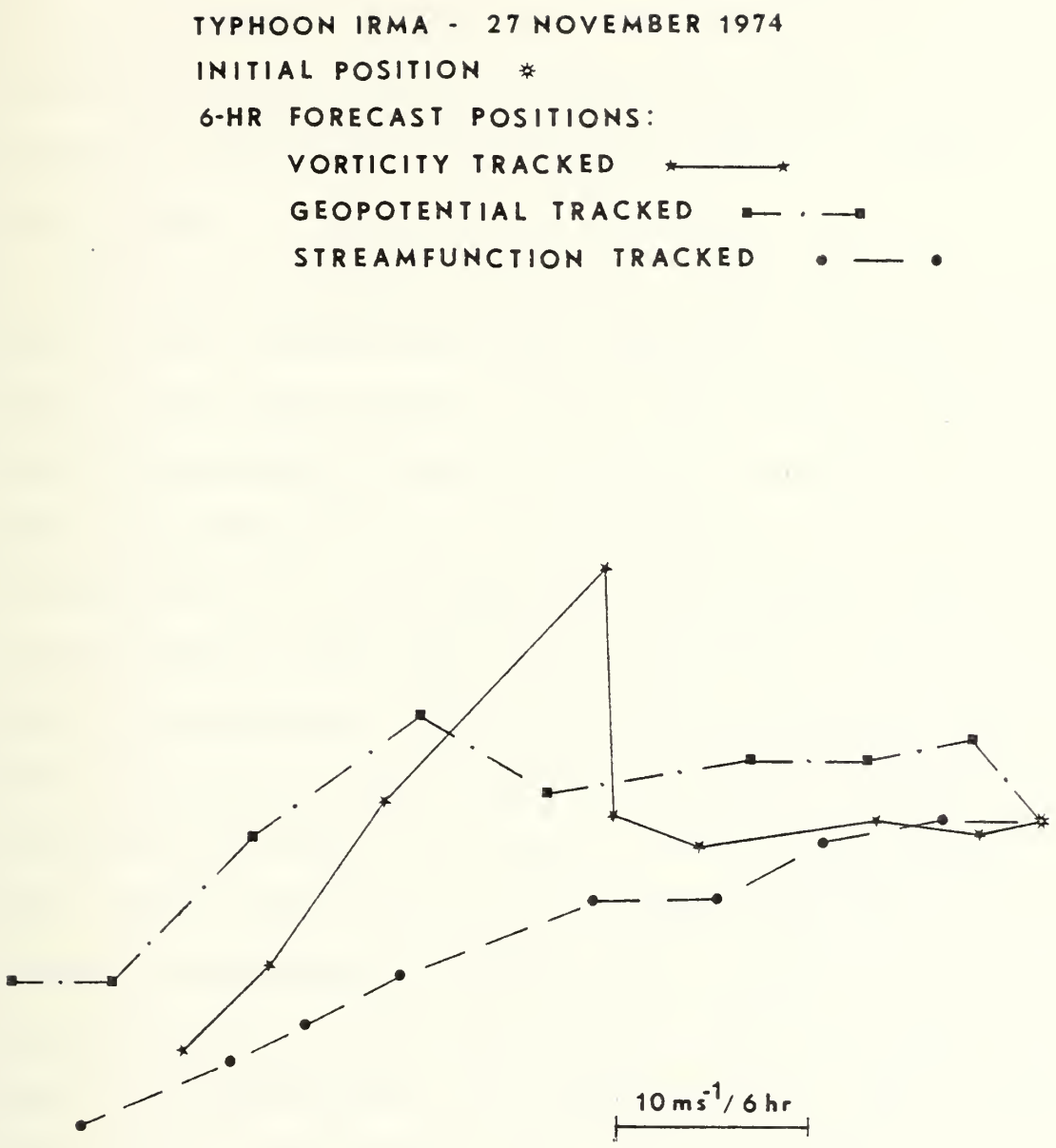

Fig. 3. Storm tracks based on vorticity, geopotential and streamfunction fields for Typhoon Irma, 27 Nov. 1974.

The second method of tracking using the 1000-mb height minimum increased tracking accuracy only slightly. The u and v components defining the anomalous vorticity centers were reflected in the ϕ fields through the equations of motion. Therefore, secondary pressure minima were also produced in the troughs.

The third method of tracking the storm with its associated ψ center achieved the most consistent estimates of the desired wind field center. These were generally within a one-half gridlength (approximately 100 km) error limit. Before calculating $\nabla^2\psi$, the forcing function (ζ) was partially a function of u', the u-component perturbation field. By eliminating the mean zonal flow, circulation centers became more easily defined. The streamfunction minimum defines a wind circulation center, whereas a vorticity center does not necessarily define a low center. Of the three methods tested, the ψ fields provided the most accurate tracking. The Sanders integrated barotropic (SANBAR) model, currently in use by the National Hurricane Center (NHC), Miami, Florida, also uses the streamfunction for tracking (Pike, 1972). SANBAR identifies a storm center with a local minimum in ψ or maximum in $\nabla^2\psi$, but in practice, the average position between the two extremes is used.

In some cases with wind speeds less than 1 ms^{-1}, the streamfunction's minimum value was also weakly defined. One might then consider a method of strengthening the gradients of ψ by artificially increasing the wind speeds across the

center location. A "biased inverse enhancement" method was tested which further increased the accuracy of locating the circulation center. This method is based on a negative, natural log function. The greatest enhancement occurs to winds less than 5 ms^{-1} (Fig. 4). Biasing the winds by a factor of 10^{-9} (this bias proved effective, although larger or smaller factors may be used depending in the degree of enhancement desired) further enhances these fields and the resulting ψ fields, with the maximum emphasis on highlighting weak highs/lows. However, these regions of very weak winds near the storm center are highly transient features within the general trough. The accurate tracking provided by this method and the limited resolution of the coarse grid TCM may result in various oscillations that are not representative of the envelope of the storm. Therefore, all results presented in this study were tracked from streamfunction fields calculated as in (3). Note that the "biased inverse enhancement" method approaches the limits of interpolating fields of finite data. The location of extraneous perturbations may not be representative of the true circulation. Since the increased resolution provided by nested-grid models can realistically depict small-scale wind fields, those circulation centers tracked by the "enhanced" method would be more meaningful.

It is of interest to note that because of these results, tracking tropical storms with ψ minima has already been incorporated into FNWC's TCM in their operational support of JTWC.

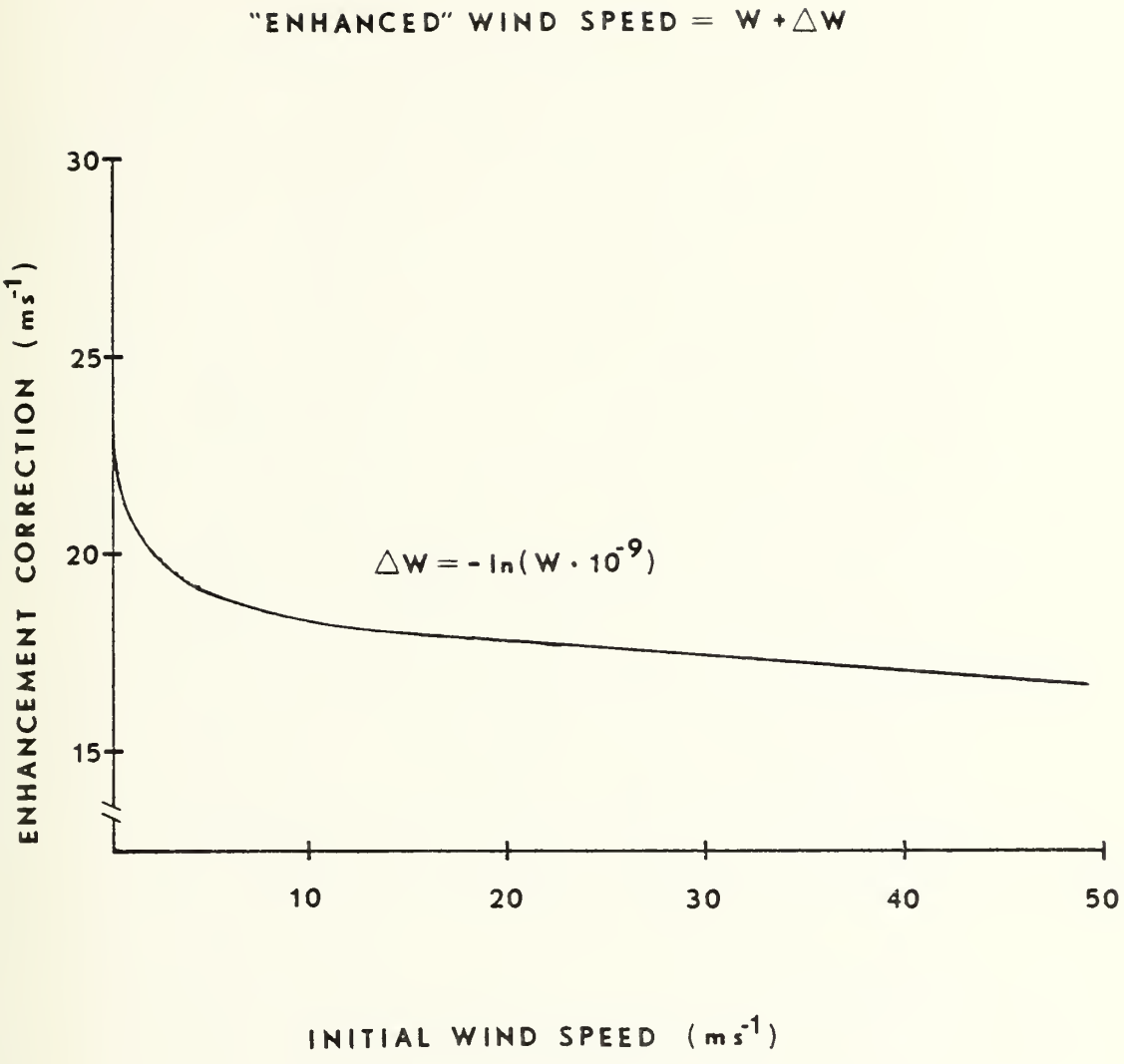

Fig. 4. Adjusted wind components at near-zero wind speeds derived from the biased inverse enhancement function (see text).

This was made possible through the efforts of Lt. D. Hinsman, USN, at FNWC, who evaluated and implemented the method.

III. INITIALIZATION

A. TROPICAL VS. EXTRATROPICAL

In general, initialization of tropical models differs from their extratropical counterparts. In a mid-latitude model, the wind is normally derived from a solution of the balance equation with an objectively analyzed geopotential field (Haltiner, 1971). Such a procedure is not suitable for a tropical model since the pressure gradient in the lower latitudes is very weak and the pressure field is not well defined. Moreover, it can be shown that the mass field primarily tends to adjust to the wind field in the tropics during the early stages of the integration after initialization, especially in mesoscale models as found by Anthes (1974). Consequently, in the tropics, primary consideration must be given to the wind field when performing the initial diagnostic phase.

A complete discussion of the theory and finite difference equations used for the TCM initialization can be found in the Appendix.

B. DATA INPUT

Wind data for the 1974 cases was supplied by the U. S. Fleet Weather Central/Joint Typhoon Warning Center, Guam, Mariana Islands (FWC/JTWC). The 850-, 500-, and 250-mb streamlines and isotachs were hand-analyzed for Typhoons

Irma and Gilda. These analyses, plus careful extraction of the data to the grid, provided a data base superior to the objective analyses used by the 1975 semi-operational cases (Elsberry, 1977). This combination of accurate hand-analyses and the directional variations of Irma (westward track) and Gilda (recurving track) provided diversified test samples. Not only did these two storms follow widely varied tracks, but the TCM forecast both good and poor tracks even though their initial data was hand-analyzed. It was therefore imperative that the biasing scheme presented should not markedly alter a good forecast.

For convenience, the hand-analyzed, synoptic data at 500- and 200-mb (800-, 700-, 400-, and 250-mb for 1975 cases) were moved to the nearest model predicted level (reference Appendix, Fig. A-1). Subsequent reference to these levels will be according to the synoptic data fields, not the model's predictive levels.

Data initialization for the 1975 cases was from the FNWC global band upper air analyses (GBUA). The bogusing of upper-level cyclonic outflow has not yet been incorporated into the initialization procedure of the FNWC TCM. For this reason, plus the incomplete assimilation of Defense Meteorological Satellite Program (DMSP) data (see Elsberry, 1977), these cases had significantly inferior upper-level circulations compared to the 1974 cases.

IV. DEVELOPMENT OF THE BIASING PROCEDURE

A. THE PROBLEM

The problem confronted by this thesis was the consistent initial forecast error of FNWC's TCM. In some cases, the error was small, but in other cases, the model forecast track deviated significantly from the most recent movement of the storm. The hypothesis is that the observational data base was inadequate in these cases, and adjustments should be made to the initial data.

The purpose of this thesis was to bias objectively the TCM's initial wind fields from the storm's recent 12-hour movement and to test this procedure on a semi-operational, real-time basis. To be discussed are the bias input, which represents the recent 12-hour movement centered on the observation time; the steering current, which interrelates the cyclone/environmental flow fields; the statistical regression equation, which predicts the TCM's storm movement; and the bias corrector and how it was applied to the TCM's wind fields.

B. THE BIAS INPUT

The vector which represents the best estimate of the recent storm motion was defined as the bias input. The bias input would, on a real-time basis, be a past 12-hour vector provided by JTWC or any operational site. The 12-hour vector

was chosen to reduce errors produced by sporadic and short-term oscillations introduced by various positioning techniques from synoptic, aircraft, and satellite data. Since FNWC's TCM begins at observation time plus 9 hours, the 12-hour vector could be centered about the observation time. For example, the bias input for a 0000 GMT observation time would begin at the 1800 GMT position from the previous day and end at the 0600 GMT position. While developing this biasing technique, best-track positions were used to insure a good bias input. In an operational mode, this vector would be derived from tropical cyclone warning positions, which would introduce some additional error. For better accuracy, a bias input consisting of a best-track position at observation time minus 6 hours and the warning position at observation time plus 6 hours could easily be developed and utilized at an operational site. If such a continually-updated tracking program were developed, the accuracy of the bias input would improve over those using only warning positions. It should be noted that the input vector is linear and therefore becomes less reliable as the true storm velocity accelerates, or changes direction rapidly.

C. DEFINITION OF THE STEERING CURRENT

Before any modification or correction could be applied to the model, a standard, cyclone/environmental wind field relationship had to be established. The proper domain of horizontally-averaged wind fields were needed to define a representative steering current. This averaged current was

needed later to estimate the difference between the actual storm track and that predicted by the TCM.

Before determining the steering current, each storm center was first assigned an origin at its nearest grid point. Second, area averages over increasingly larger domain sizes were calculated to find a consistent and representative wind field relating cyclone motion to environmental flow. These domain sizes ranged from 3 x 3 to 13 x 13 grid squares centered on the storm. To simplify the problem, wind averages from each level (850-, 500-, and 250-mb) were added to define the vertically-averaged steering current.

Averaged u and v components as a function of increasing domain are depicted in Fig. 5 for the 1974 (hand-analyzed) cases. Note that the averages show a weak, positive v component and a strong, negative u component reflecting the general WNW movement of tropical cyclones. Averaging over larger areas should tend to decrease the effect of the dominant typhoon circulation, with the result being the steering current. The ideal average would produce a slope rapidly decreasing with increasing area indicating a region beyond some zone where the component averages become invariant. This zone would be equally influenced by the cyclone/environmental flow fields. This zone is evident from the 850-mb's u and v components (Fig. 5) near the 7 x 7 (12 degree) square which is approximately equal to a circle with a $6\frac{1}{2}^{\circ}$ radius. Jones (1976) also observed this zone at a radius of about 600 km using a triply-nested model with a middle grid

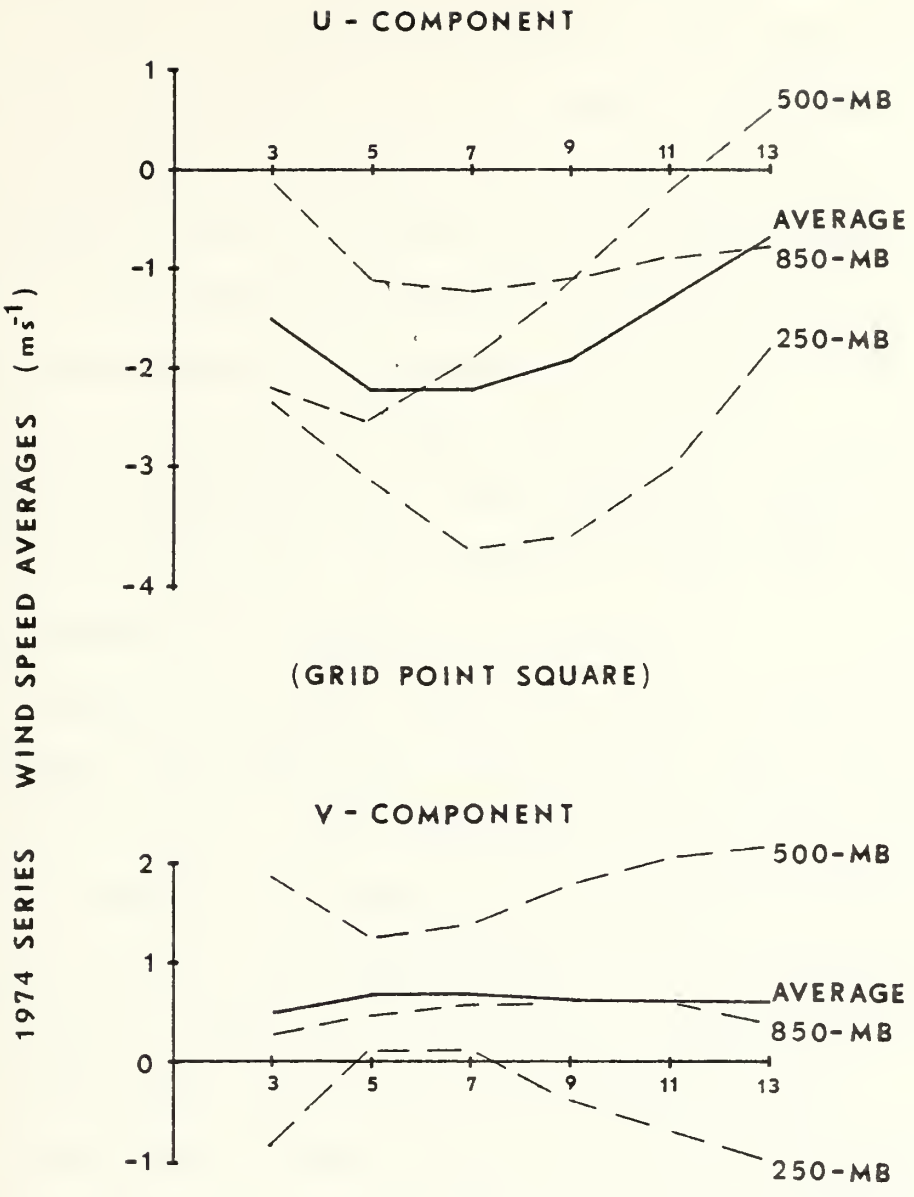

Fig. 5. Average u and v components over successively larger domains for three levels based on the 1974 cases.

resolution of 30 km. Similar results were obtained by George and Gray (1976) by averaging rawinsonde data from nearly 200 typhoons within concentric, radial bands. They found that the most consistent averages relating storm movement and speed to surrounding winds lie within the 1-7 degree radial band. It appears that behond this zone, the influence of the shear in the environmental flow becomes more dominant. This 6-7 degree "zone of influence" best delineates the cyclone/environmental flow characteristics. The component slope reversals within this zone become better defined with height, with the sharpest reversal at 250-mb.

The component averages depicted in Fig. 6 were based on non-divergent wind components derived from the FNWC global band wind analysis. (Note that the hand-analyzed cases were similarly treated.) The main difference between these fields and those from the hand-analyzed winds is the absence of the slope reversal, except for the 500-mb u component. Only the 850-mb components resemble the hand-analyzed cases. This may be attributed to FNWC's bogus initialization, which is most realistic at the lowest level, but weakens with height (see Elsberry, 1977). Due to the higher reliability placed on the hand-analyzed cases (Fig. 5), along with similar results from previous studies, all the area-averaged steering currents hereafter presented were calculated for a 7 x 7 (approximately 12 degrees longitude) square centered on the storm.

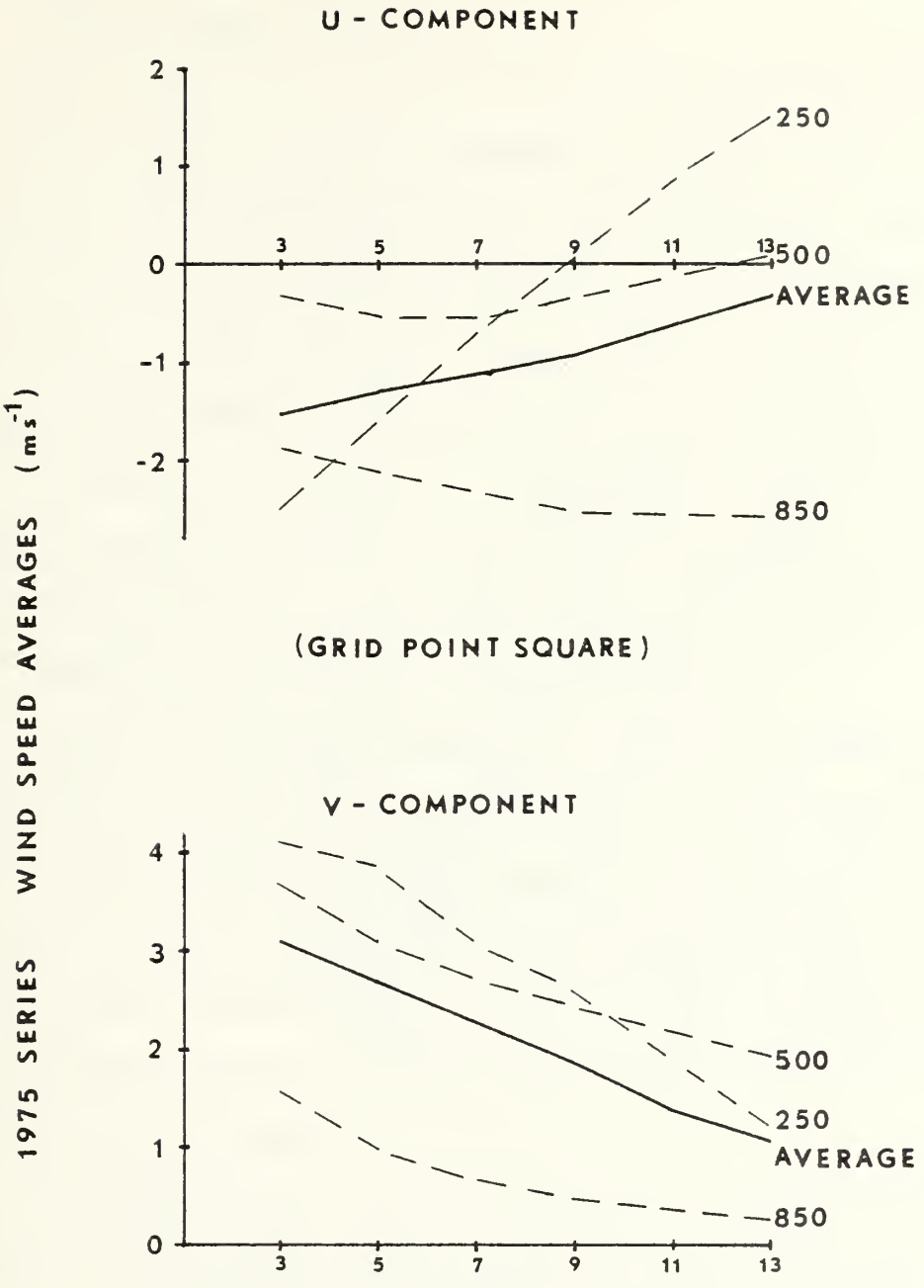

Fig. 6. Same as Fig. 5 except for '1975'.

D. ESTIMATION OF THE EXPECTED MODEL STORM MOTION

1. Initial Observations

Given the actual storm motion during the first 6 hours of the forecast period, one must estimate the expected model storm track to determine the bias corrector that should be applied to the initial data fields. Running the model for approximately 6 hours would be ideal, but this would increase computer requirements. A plausible alternative may be to predict the model storm initial movement based on a number of prior case studies. Thus, a statistical regression equation was generated to estimate initial storm movement given the initial steering currents in the three layers.

Development of the regression equation began with observing the initial 6-hour TCM vector of each test case. A 6-hour vector was chosen since maximum emphasis was placed upon improving the initial TCM storm movement. This vector had to be small enough to be correlated with the instantaneous steering current and yet large enough to represent the trend of initial storm movement.

Hodographs depicting the average velocity vectors considered in the regression equation's formulation are shown in Figs. 7 and 8. One may compare the steering currents for each level, and the vertical mean current, with the TCM's 6-hour vector and the corresponding 6-hour best track vector. This latter vector is essentially the last 6-hour segment of the 12-hour bias input. All vectors were normalized with respect to the model storm vector which was prescribed to be

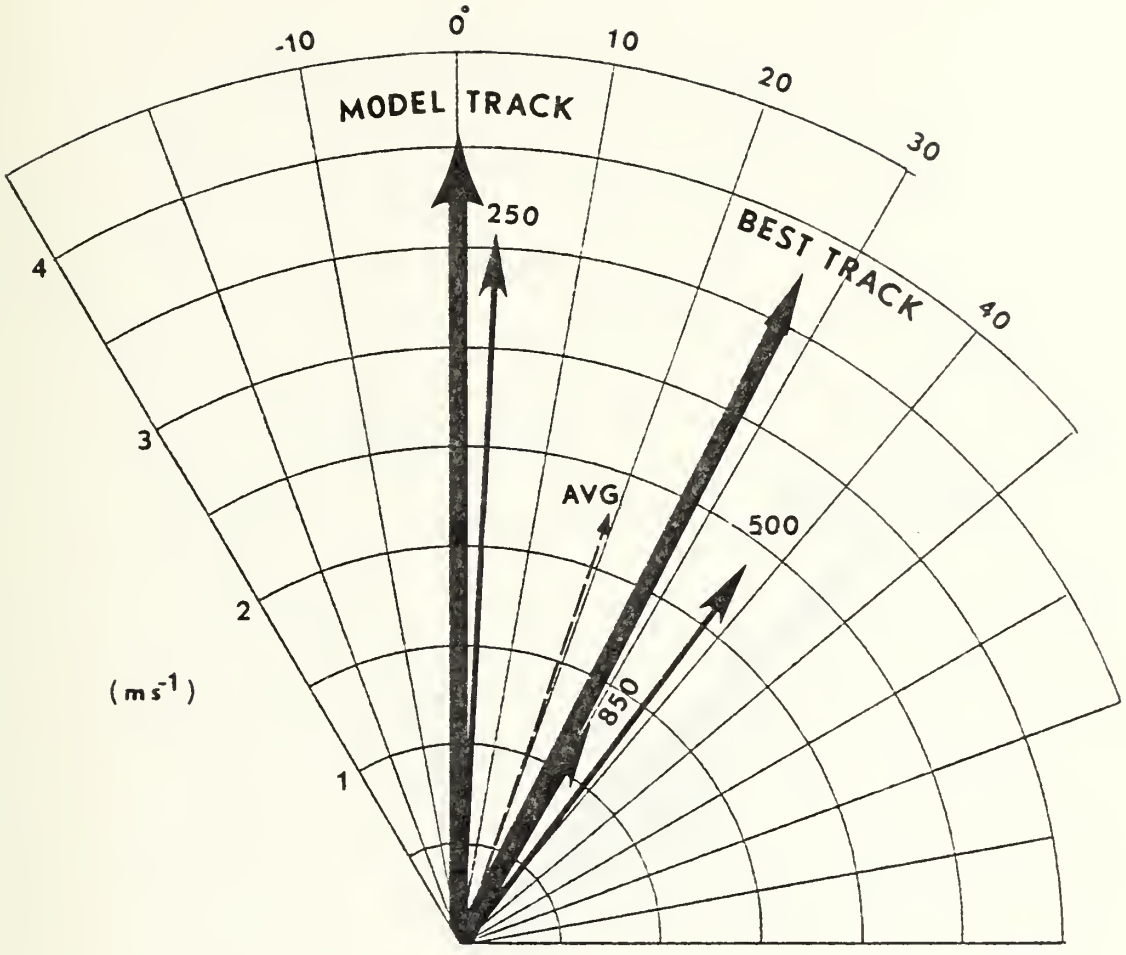

Fig. 7. Average initial steering currents, best track and model storm motion in first six hours for the 1974 cases.

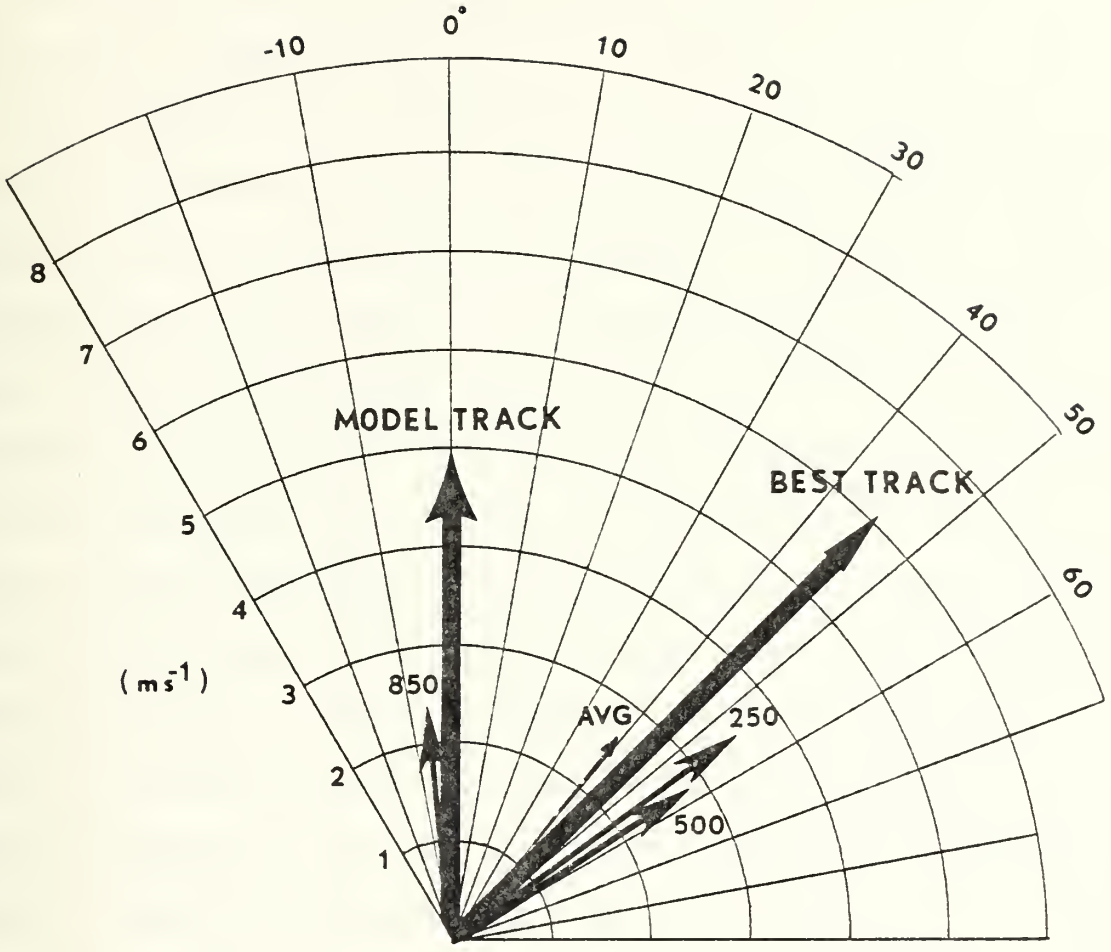

Fig. 8. Same as Fig. 7 except for '1975'.

at 360°. Some of the results were surprising. The first anomaly revealed by Figs. 7 and 8 is the lack of alignment between individual steering currents and the actual path of the storm. Comparison of the two figures shows that the 500-mb currents have relatively similar relationships to the currents above and below. But the currents at this level were also most consistent with respect to individual cases. Comparison of the other levels revealed data differences. The reverse relationships of the 850- and 250-mb currents between the 1974 and 1975 cases were probably due to the use of hand-analyzed data in the 1974 cases, while the 1975 cases were derived from objectively-analyzed data. Specifically, the typhoon bogus applied in the 1975 cases resulted in relatively good flow fields at low levels, but poor fields aloft. The 1974 cases, on the other hand, exhibited superior upper level analyses due to the inclusion of aircraft and subjectively derived satellite data.

The second characteristic common to Figs. 7 and 8 is that the model storm traveled about twice the speed of the averaged steering current. However, beyond the 6-h forecast periods, the TCM speed forecasts were too slow relative to the best track. The 1975 case steering currents were also slow (about 2.6 ms^{-1}), which can be attributed to the objective analyses. The vertical structures of the steering currents in the 1974 series appear to be more realistic. The individual steering current speed became greater with altitude and nearly matched the model's speed at 250-mb.

This observation suggests the importance of the upper level steering currents for short-term motion forecasts and emphasizes the need for greater quantity and better quality upper-level data.

An alternative method of biasing was also investigated. The recent study by George and Gray (1976) produced an empirical relation between the storm track and a steering current (mean flow) derived from rawinsondes. Their research included stratifications of the data according to storm latitude, translation speed and direction, intensity, and intensity changes with respect to the surrounding winds. The hodograph in Fig. 9 depicts their averaged empirical steering current relative to the storm's actual movement. It is important to note that the empirical steering vector was taken to be 86% of the mean 700-mb speed and 16° to the right of the mean 500-mb direction. Notice the comparison between the averaged steering currents from Figs. 7 and 8 and George and Gray's mean flow, which is essentially the storm steering current. This mean empirical vector and the 1974 averaged current have nearly identical angular displacements with the latter being 30% slower. This close agreement was to be expected, since both vectors were constructed from raw data relationships, although the methods differed. The 1975 objective analyses, however, produced an averaged current that had twice the angular displacement and was 33% slower than George and Gray's mean empirical vector.

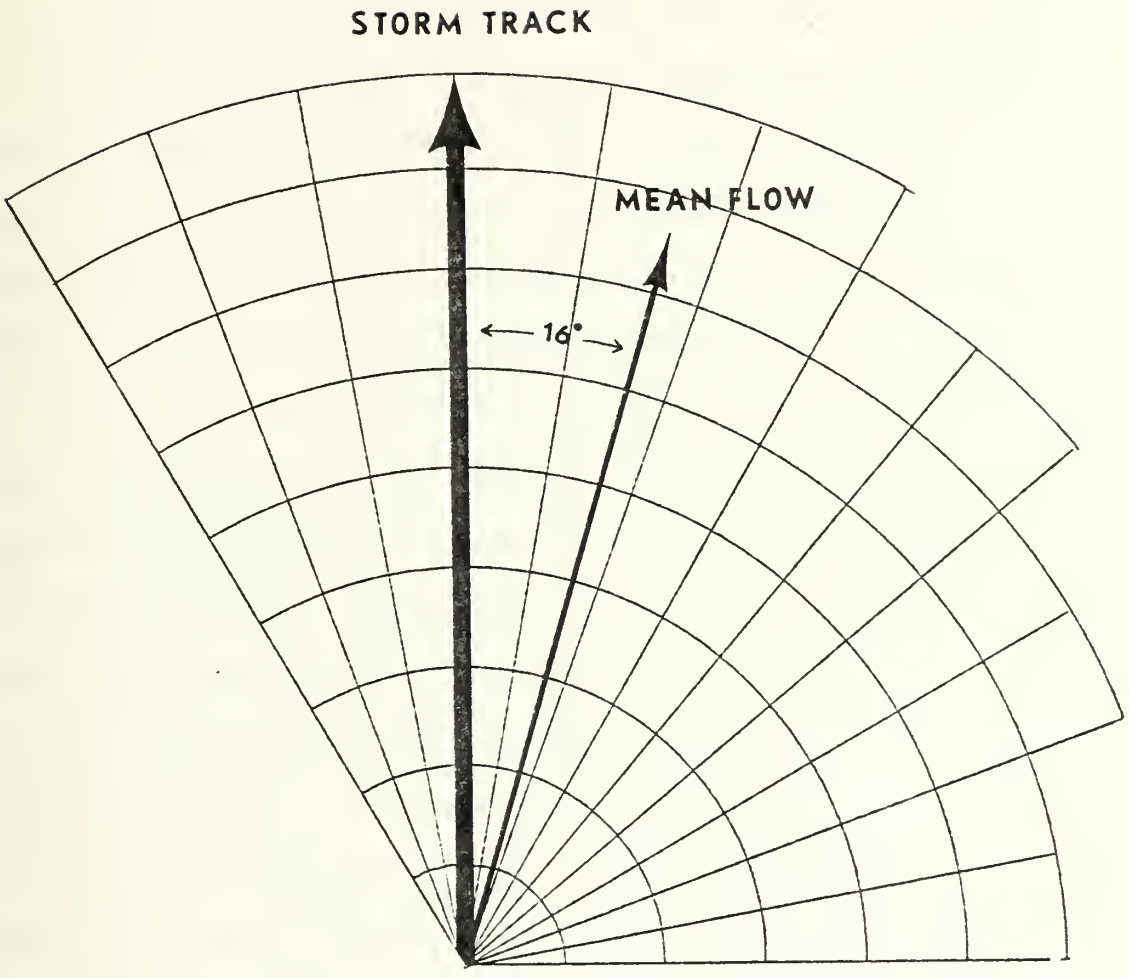

Fig. 9. Empirical mean flow relationship with respect to actual storm motion vector based on George and Gray (1976). Mean flow is 86% of 700-mb speed and 16° to the right of 500-mb direction.

2. Model Characteristics

Experimental adjustments designed to alter the steering currents by biasing the wind fields were first done with the hand-analyzed cases. It was found that the boundary conditions used for the TCM's initialization process (see Appendix), for the derivation of ψ and subsequent non-divergent wind fields, distinctly changed the resulting steering currents. These adjustments altered significantly major portions of the flow fields. Comparison of Fig. 10 (original 850-mb wind field) and Fig. 11 (non-divergent 850-mb wind field) reveals the distinct boundary effects characteristic of this "channeled" model. New steering currents calculated after this initialization are presented in Figs. 12 and 13. Comparison with the corresponding divergent steering currents (Figs. 10 and 11, respectively) illustrates the changes. The effects of deriving the non-divergent components of the 1975 cases were significant. Even larger vector changes occurred with the 1974 cases. The hand-analyzed fields contained strong convergence/divergence areas, which were completely removed. An overall reduction of wind speeds was consistent with all cases studied. The dramatic differences between Figs. 8 and 13, and especially Figs. 7 and 12, dictate strongly that the steering currents must be calculated from non-divergent wind components to accurately reflect the storm/environmental relationships within the model.

3. The Prediction Equations

The purpose of the prediction equations as applied to the 1974 and 1975 cases was to estimate the initial storm

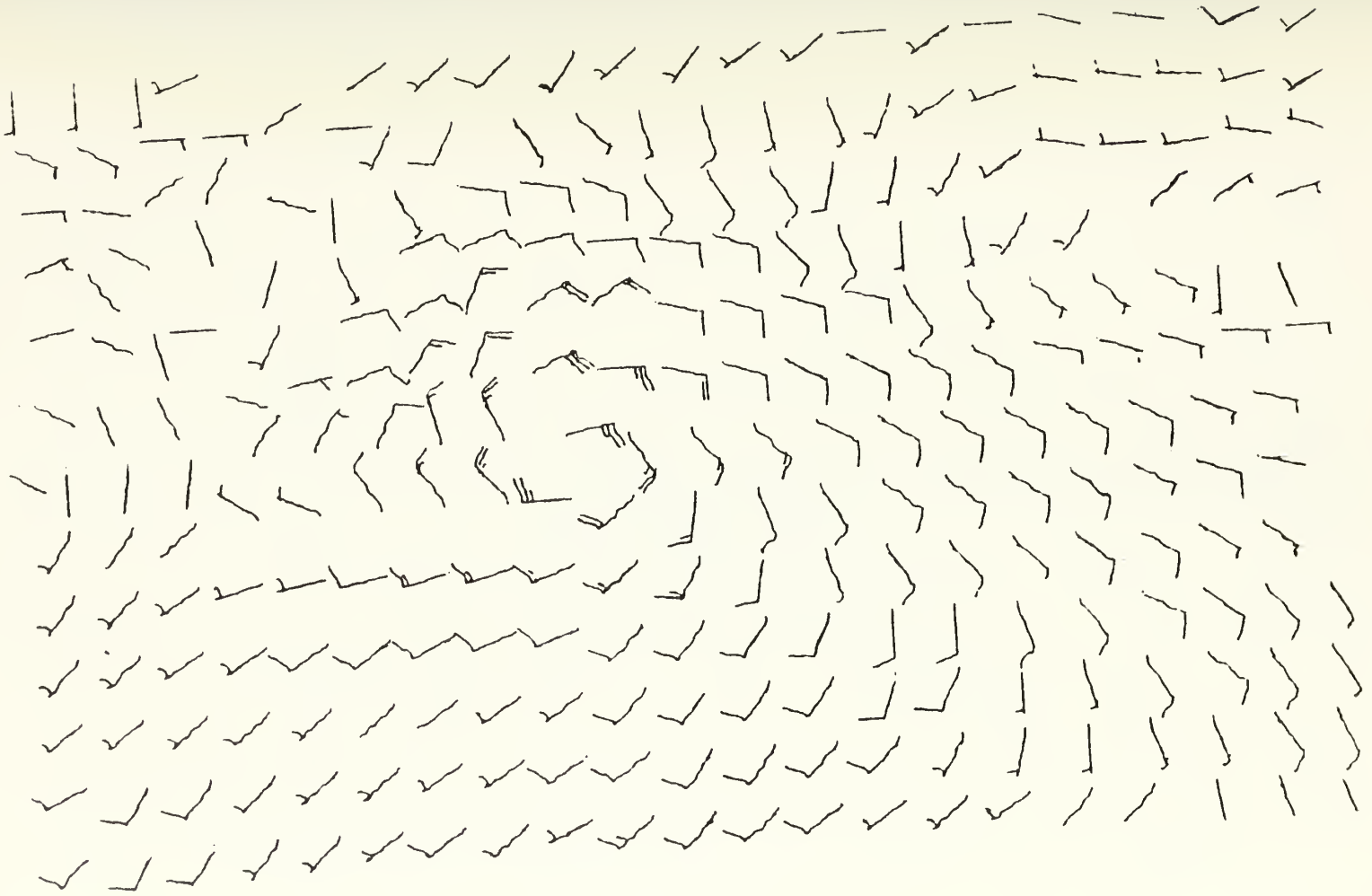

Fig. 10. 850-mb wind field for Typhoon Gilda, 04 August 1974.

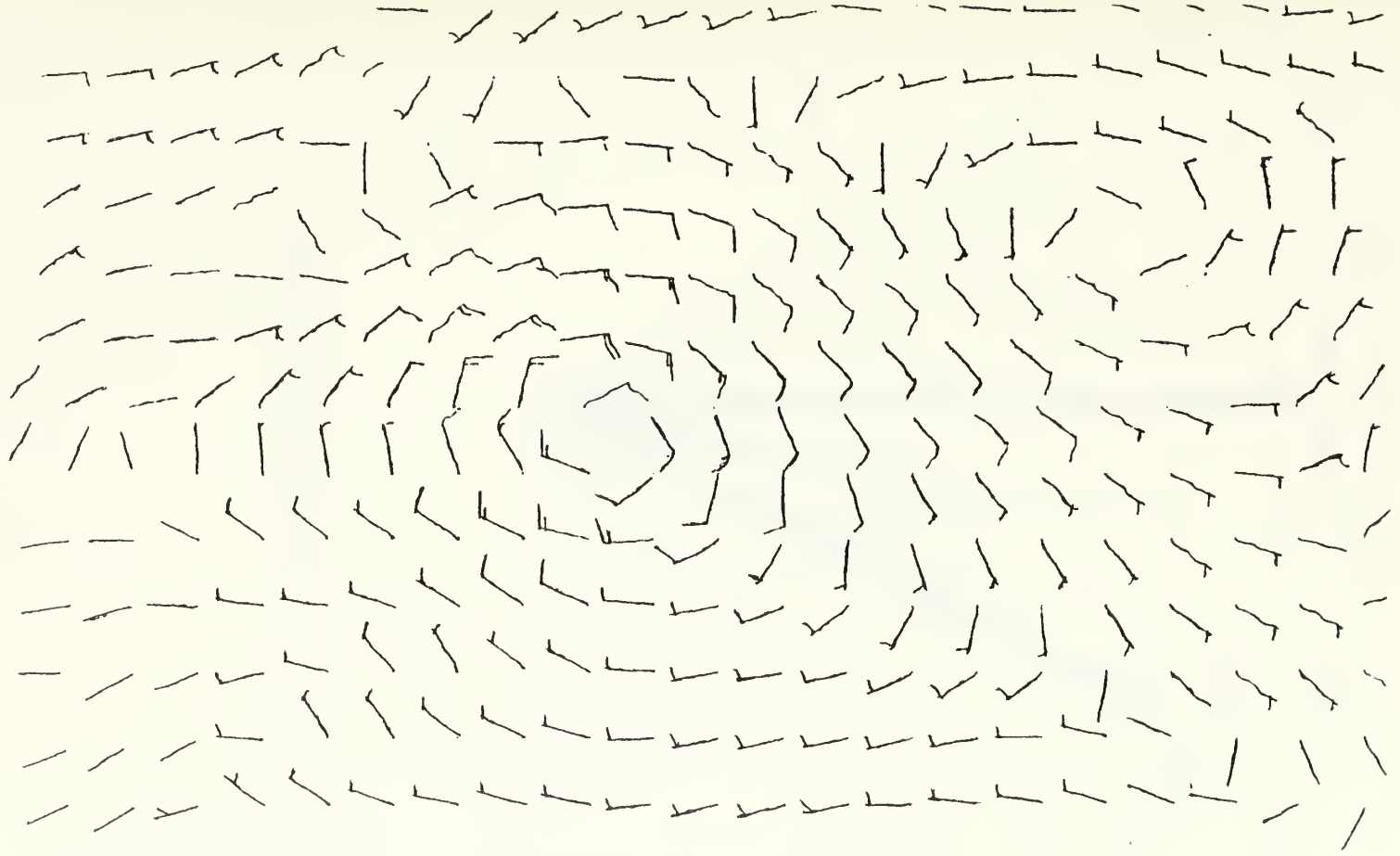

Fig. 11. Non-divergent winds at 850-mb for same field as in Fig. 10.

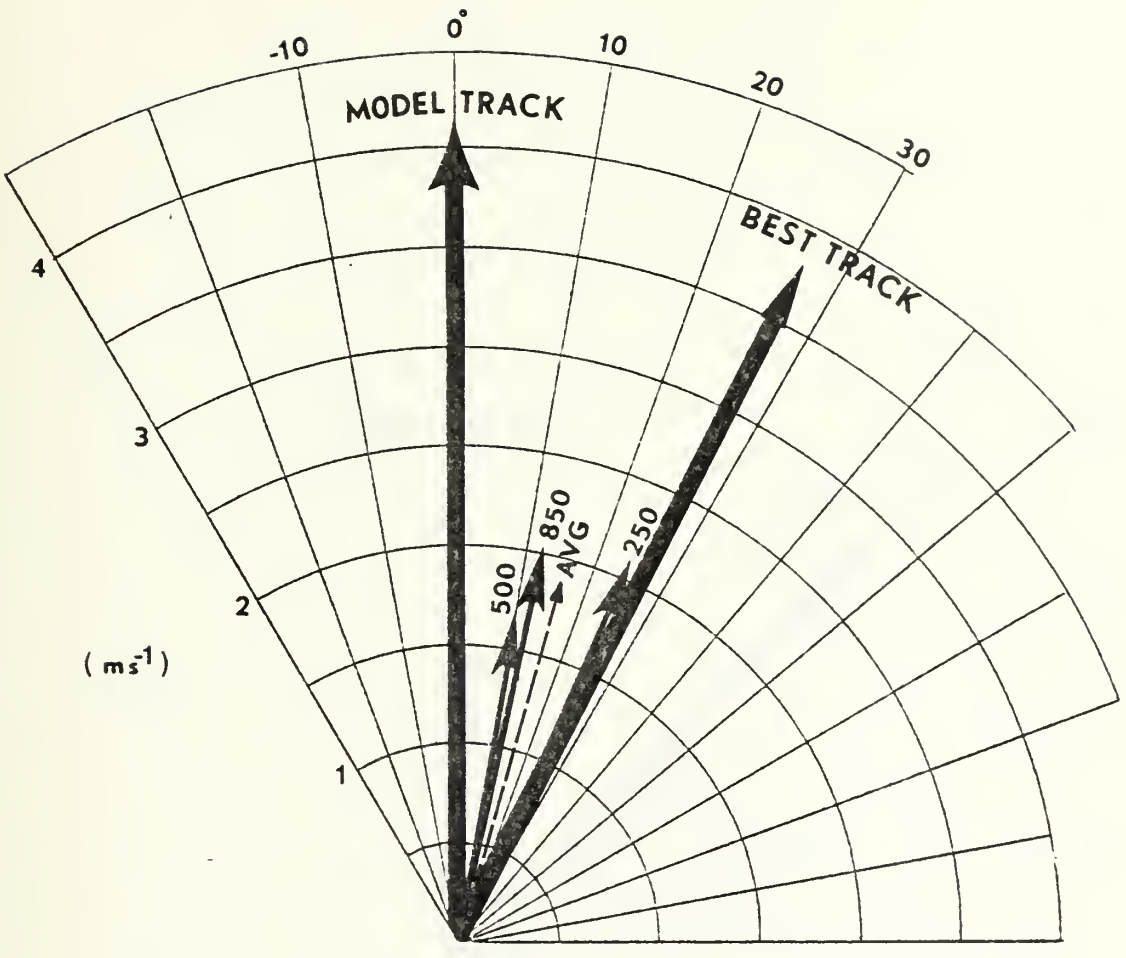

Fig. 12. Same as Fig. 7 except with steering currents based on non-divergent winds.

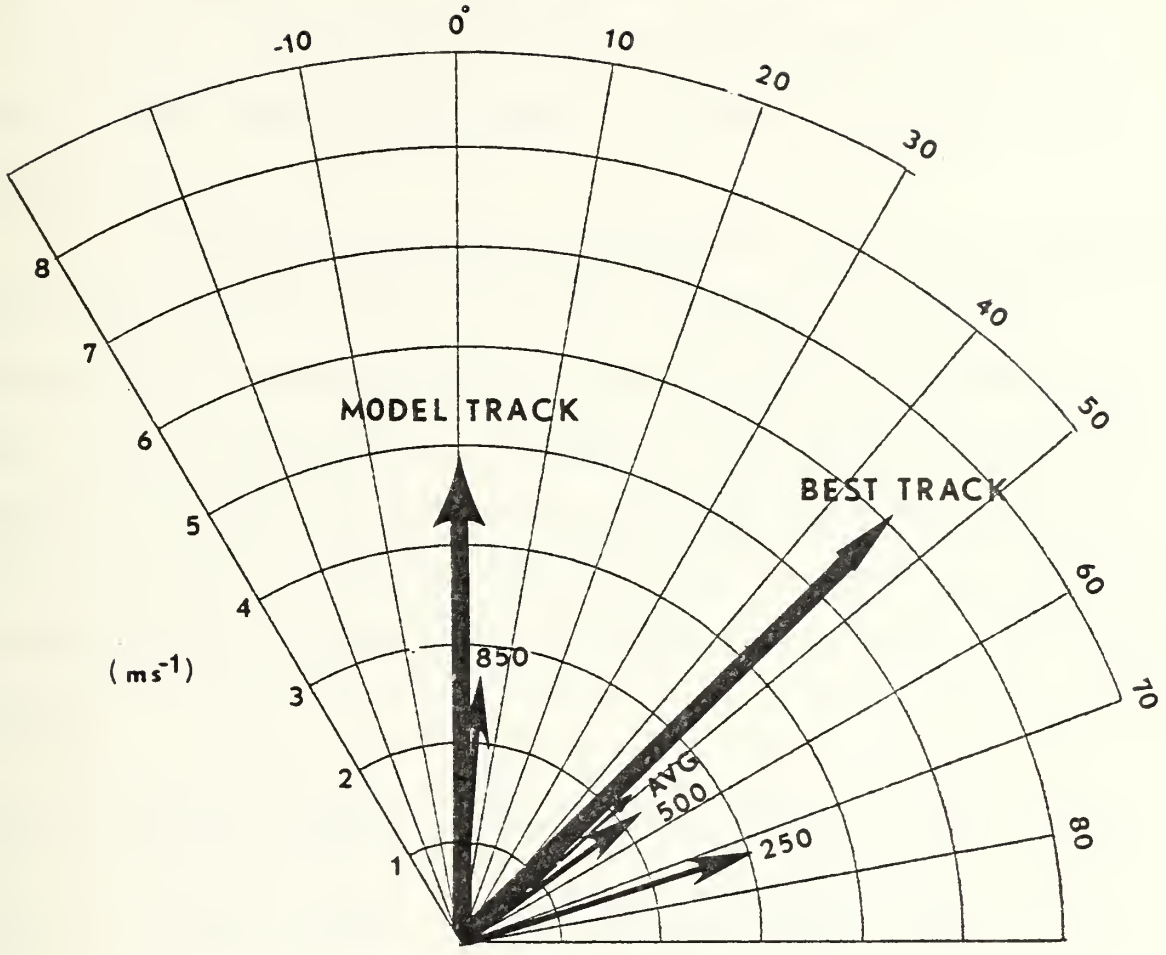

Fig. 13. Same as Fig. 8 except with non-divergent winds.

movement in the TCM from the initial steering current information. Statistical regression coefficients were calculated with a Bio-Medical Stepwise Regression program (Dixon, 1975). By contrast, the second adjustment method based on George and Gray (1976) came directly from the vector relationships presented in Fig. 9.

To obtain the maximum information from the individual steering currents, all the u and v components were used as independent variables (4a, b). The predicted components of the initial storm motion (U_M and V_M) were sums of their constants (CU and CV, respectively) and the products of their six steering u, v current components and respective regression coefficients (A through F). Numbered subscripts denote model layer.

$$U_M = CU + A_u U_{850} + B_u U_{500} + C_u U_{250} + D_u V_{850} + E_u V_{500} + F_u V_{250} \quad (4a)$$

$$V_M = CV + A_v U_{850} + B_v U_{500} + C_v U_{250} + D_v V_{850} + E_v V_{500} + F_v V_{250} \quad (4b)$$

High confidence levels were found for the 1974 coefficients with the regression equations explaining 100% and 99% of the predicted u and v (respectively) storm components. The hand-analyzed data proved highly reliable even with the steering currents averaged from the non-divergent winds. The 250-mb v component alone explained 72% of the predicted V_M component. It must be noted that only seven hand-analyzed cases were available to produce these coefficients with such high confidence. More cases may have reduced their reliability. The confidence levels of the 1975 coefficients were less than

those of the 1974 cases. These coefficients explained 78% and 68% of their respective U_M and V_M variances. The decreased effectiveness of the 1975 coefficients can partially be explained by the inferior wind fields initially supplied to the TCM, again emphasizing the need for an improved cyclone bogus and the lack of better data for and analyses from the GBUA. In addition, the greater number of cases (41) explained by these coefficients would also account for their ineffectiveness relative to the seven 1974 cases.

The two vectors depicted by Fig. 9 provided the necessary relationships needed to formulate an empirical equation based on the George and Gray results. This equation, however, derives a mean flow from the bias input, not storm motion. The consolidated empirical vector, representing fractions of the 700-mb speed and 500-mb direction, was utilized as a vertically averaged steering current. This was necessary since the derived mean flow needed to be compared to the observed, vertically averaged steering current. A mean flow vector was then derived from the bias input, which represents the best track vector (Fig. 9), and the empirical relationships defining a corresponding storm mean flow (5a, b).

$$\text{Empirical Mean Flow Speed} = 86\% \times \text{Bias Input Speed} \qquad (5a)$$

$$\text{Empirical Mean Flow Direction} = 16^{\circ} + \text{Bias Input Direction} \qquad (5b)$$

The bias input and its derived mean flow then reflected the identical relationships displayed by Fig. 9.

E. THE BIAS CORRECTORS

1. First Approach

A bias corrector is defined as the correction applied to a wind field to adjust the steering current to conform to the desired storm motion (Fig. 14a). For the 1974 and 1975 storms, their initial motion was predicted from a regression equation. The bias correctors, Δu and Δv (defined by Eq. 6a, b), are

$$\Delta u = \text{Bias Input } (u) - U_M \qquad (6a)$$

$$\Delta v = \text{Bias Input } (v) - V_M \qquad (6b)$$

the difference between their respective component bias inputs and predicted storm motion. These correctors were then applied to their respective component wind fields for steering current adjustments as discussed in the next section.

2. Second Approach

The relationships produced by George and Gray (Fig. 9) enabled derivation of a bias input's mean flow. Since a mean flow vector represents a vertical average, the derived mean flow and observed steering current components ($\overline{U}$ and $\overline{V}$) were comparable. Thus, any differences between the two vectors (7a, b) represented the bias correctors needed to adjust the observed current to resemble the empirical current (Fig. 14b).

$$\Delta u = \text{Empirical Mean Flow } (u) - \overline{U} \qquad (7a)$$

$$\Delta v = \text{Empirical Mean Flow } (v) - \overline{V} \qquad (7b)$$

An important difference between the derivation of the two sets of bias correctors is that the "storm track" derived

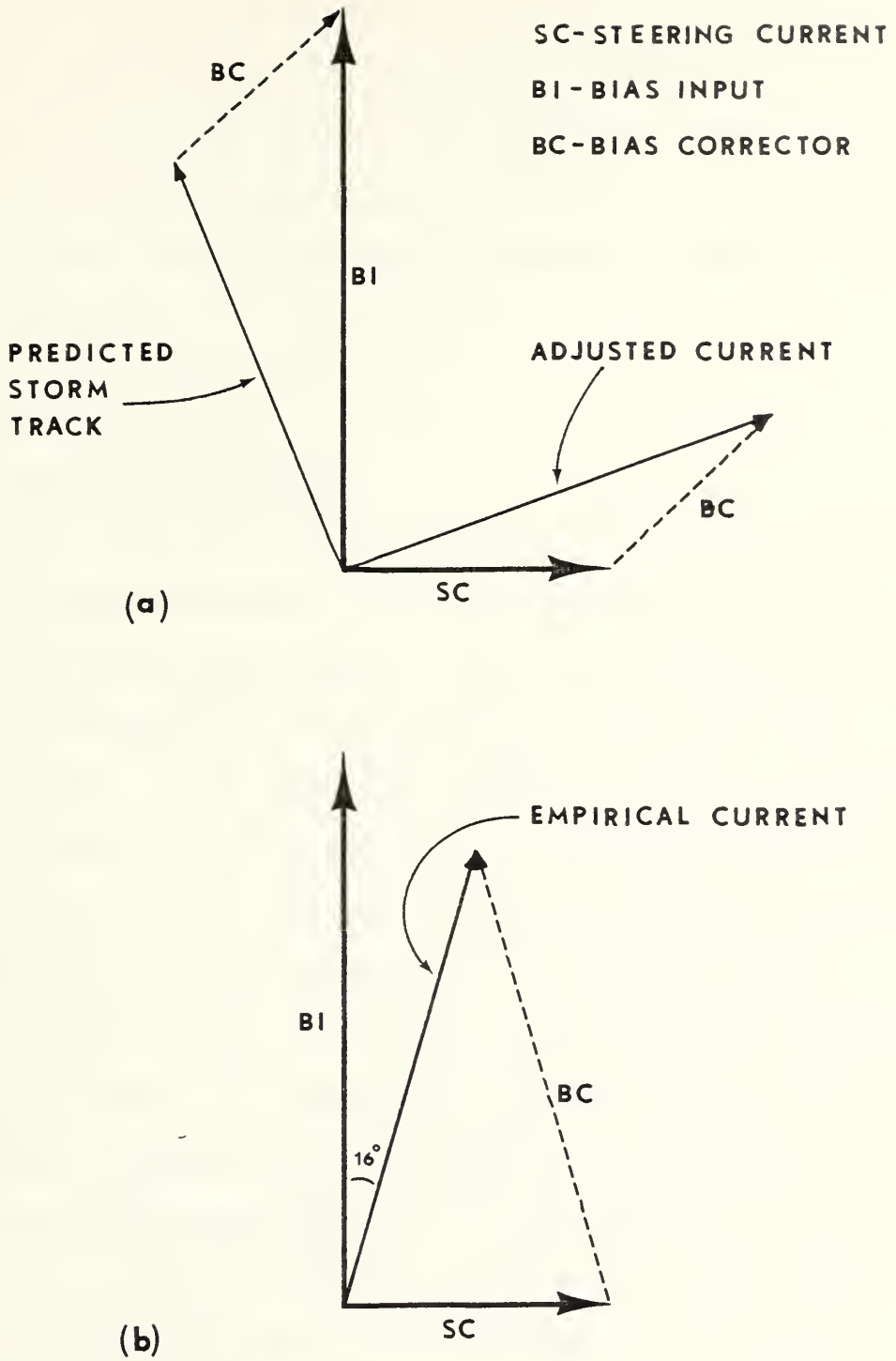

Fig. 14. Schematic of the bias corrector definition from (a) the first approach using the predicted initial storm motion and (b) second approach using the empirical steering current.

correctors (first approach) are differences between observed and predicted storm motion, whereas the "mean flow" derived correctors (second approach) are differences between the observed and empirical mean flow. Both sets of correctors, however, adjusted the wind fields to produce a desired steering current average.

F. THE BIASING SCHEME

1. Initial Experiments

Once the bias correctors were calculated, an effective method of applying them to the wind fields was investigated. Although the steering currents varied in the three layers, adequate information to differentially bias each level was not available. Therefore, the biasing scheme was simplified by distributing the bias correctors equally in each of the three layers. If a vertically dependent biasing scheme could be developed, improved forecasts may possibly result.

First attempts at adding the derived bias correctors uniformly to the u, v fields over the entire area were not successful. Adding a uniform north-south component is inconsistent with the requirement for non-divergence in the initial wind fields. It was therefore necessary to limit the biasing domain. The logical area would be that which originally defines the steering current, a 7 x 7 grid square. The improvement in track forecasts obtained with the bias applied in a box-like function over the exact domain defining the steering currents (Fig. 15a) was rather small. Several modifications were then tried by applying the maximum bias at the

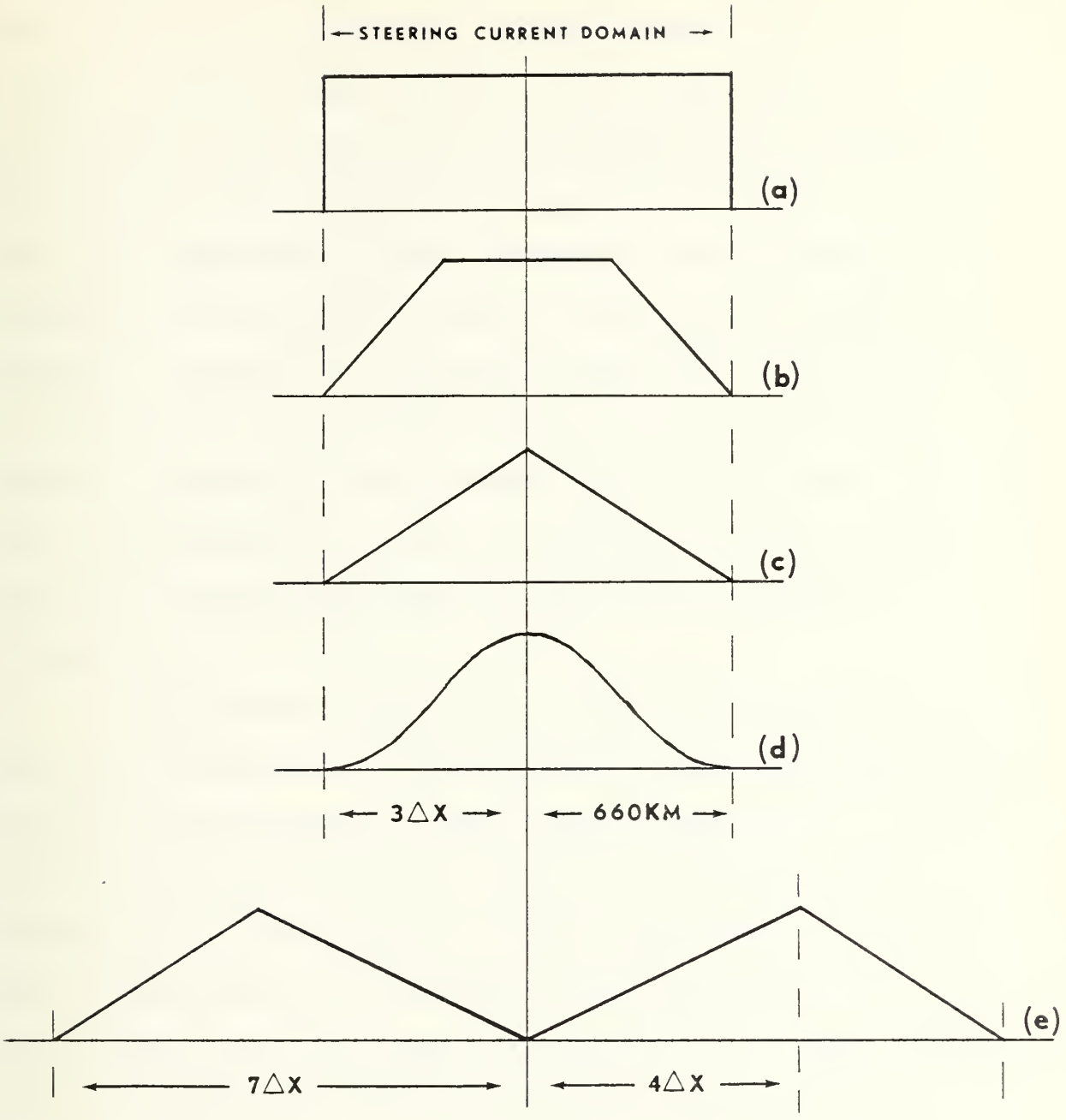

Fig. 15. Examples of various horizontal distributions of the bias corrector with respect to the grid point nearest the storm center. In each case a unit value corresponds to the desired bias corrector as in Fig. 14.

storm center, and decreasing the magnitude to zero at three grid points from the center. Varied biasing functions from linear to cosine (Figs. 15b, c, and d) were tried in an effort to eliminate the discontinuities believed to have adversely affected the wind fields by the box-like function. In addition, the magnitudes of the corrections were systematically varied with each function tried. These efforts proved unfruitful as many of the forecast tracks were ill-behaved, and in some cases, the tracking routine could not follow the center. Analysis of the forecast wind fields showed that the bias had altered the vortex so drastically that its basic structure was not maintained during the initialization processes.

The two-fold objective of adjusting the steering current and retaining the vortex indicated that the modification should be concentrated in the "zone of influence". The zone of influence was previously defined as the region about a vortex which is affected by both the storm and the environment. Application of the maximum bias just beyond the zone of influence (Fig. 15e) proved most effective. Many variations in placement of the maximum bias finally resulted in the form shown in Fig. 15e, where the maximum bias was at the fourth grid square. Although the correction values applied to this function were later modified, the placement of maximum bias was kept fixed. As an illustration of the effects of the modified biasing form used (described in Results section), the response of the wind fields to this type of biasing is apparent upon comparison of the unbiased 850-mb winds in

Fig. 11 and the biased winds in Fig. 16 for the 4 August 1974 case. The major effect was the alteration of the system's zone of influence. The winds near the vortex center underwent minor change, but the flow region (zone of influence) interacting with the surrounding flow resulted in maximum change. In this case, the surrounding flow patterns were altered significantly. The biasing literately reformed the adjacent pressure systems to insure the storm's northward movement. This was the result of the substantial bias applied, combined with the restrictions imposed by the model's boundary conditions. Although seemingly excessive, these biased wind fields resulted in significant improvement in the track forecast, as will be discussed in detail in the Results section.

Because the bias introduced both vorticity and divergence in the initial wind fields, a second streamfunction solution must be calculated to generate non-divergent wind components. However, this result deviated from the desired steering currents. Comparison of the biased and subsequent non-divergent fields revealed wind speed reductions as great as 50% in regions of maximum bias. This phase of the TCM initialization consistently decreased the magnitude of the bias by blending sharp gradients and eliminating convergent/divergent patterns introduced by the bias. Therefore, to counteract these effects, the biasing scheme was applied twice. That is, after the original initialization and calculation of the bias correctors, biasing and reinitialization was repeated. This method improved the forecasts, whereas

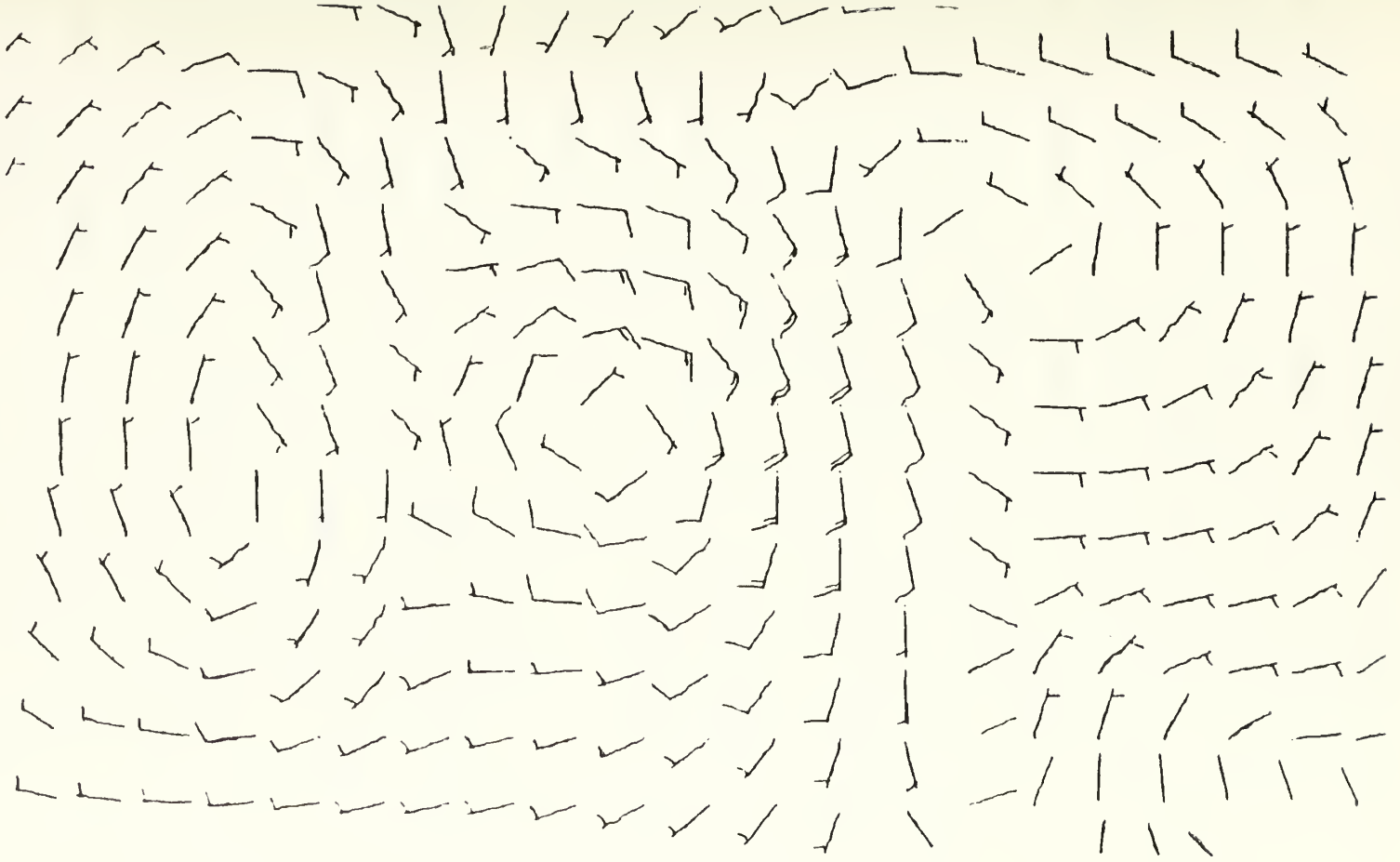

Fig. 16. Same as Fig. 11 after application of the bias corrector.

additional applications of the bias altered significantly the winds and did not result in consistent improvements.

2. Differential Adjustments

The procedures performed in this section were purely developmental. The basic method was trial and error. These steps were essential since the characteristics of each TCM (1974 versus 1975) are highly dependent on the latitudinal domain. This is a direct consequence of the no-flux conditions imposed on the north-south boundaries. The TCM domain is not relocatable during the prognostic phase. In some cases, the channel walls restricted northward movement as opposed to westward movement. The average model storm track in the 1974 cases without biasing was 269°, while the average best track direction was 296°. Corresponding values for the 1975 cases were 293° and 338°. Thus, one of the effects of the bias adjustment is to offset this model-related hindrance to the north-south storm motion.

The method employed to overcome these north-south restraints was differential component corrections. Beginning with the basic biasing function of Fig. 15e, the amplitude was systematically varied. Each 48-hour test forecast was plotted against the unbiased track and the best track. The ultimate goal of the biasing was to obtain an initial six-hour track nearly parallel to the best track without producing an unrealistic 48-hour track. At the minimum, the biasing should result in a track that matched the unbiased forecast.

The first bias application, as in Fig. 15e, used the original bias correctors Δu and Δv for the maximum values,

or the "peak" values. Then, holding the peak u-component constant, the peak v-component was either increased or decreased until the best solution was observed for the seven cases tested. Finally, the new peak v-component was held fixed as the peak u-component was varied. This process was repeated several times until no further improvements were observed.

During the development of the biasing function illustrated in Fig. 15e, it became apparent that the v-component bias would have to be much larger than the u-component to offset the TCM's north-south boundary conditions. The relative magnitudes and peak values of the u, v bias correctors were different for the 1974 and 1975 cases, for each used a different domain size. It might be anticipated that the replacement of the channel boundary conditions with a relocatable model with open boundaries would eliminate some of these problems. There should also be little or no need for differential component biasing.

V. RESULTS

A. THE 1974 CASES

The main purpose in tests with the 1974 cases was for preliminary development of the biasing scheme. Results from these cases will be presented on a relative improvement basis only. Although there were small errors associated with the initial positions, they were subtracted from all results presented. However, these errors will be included with the 1975 results as operational feasibility is examined.

The 1974 cases provided an excellent sample because the data were hand-analyzed and the statistical regression coefficients resulted in very accurate estimates of the initial model storm motion. These cases were therefore used for preliminary testing which finally resulted in the basic biasing function of Fig. 15e, as described above. An example of the results thus far is shown in Fig. 17. Because the original unbiased forecast was so poor, this case (Typhoon Gilda, 04 August) was of special interest. These TCM forecasts were plotted every 6 hours to illustrate the temporal stability within the model and the short-term effects of the various biasing functions. The unbiased 48-hour track is labeled as B in Fig. 17, and may be compared to the best track (A). The first attempts with the box-like, cosine and basic biasing functions are shown in tracks C, D and E. The maximum values applied to the functions were the unit Δu, Δv

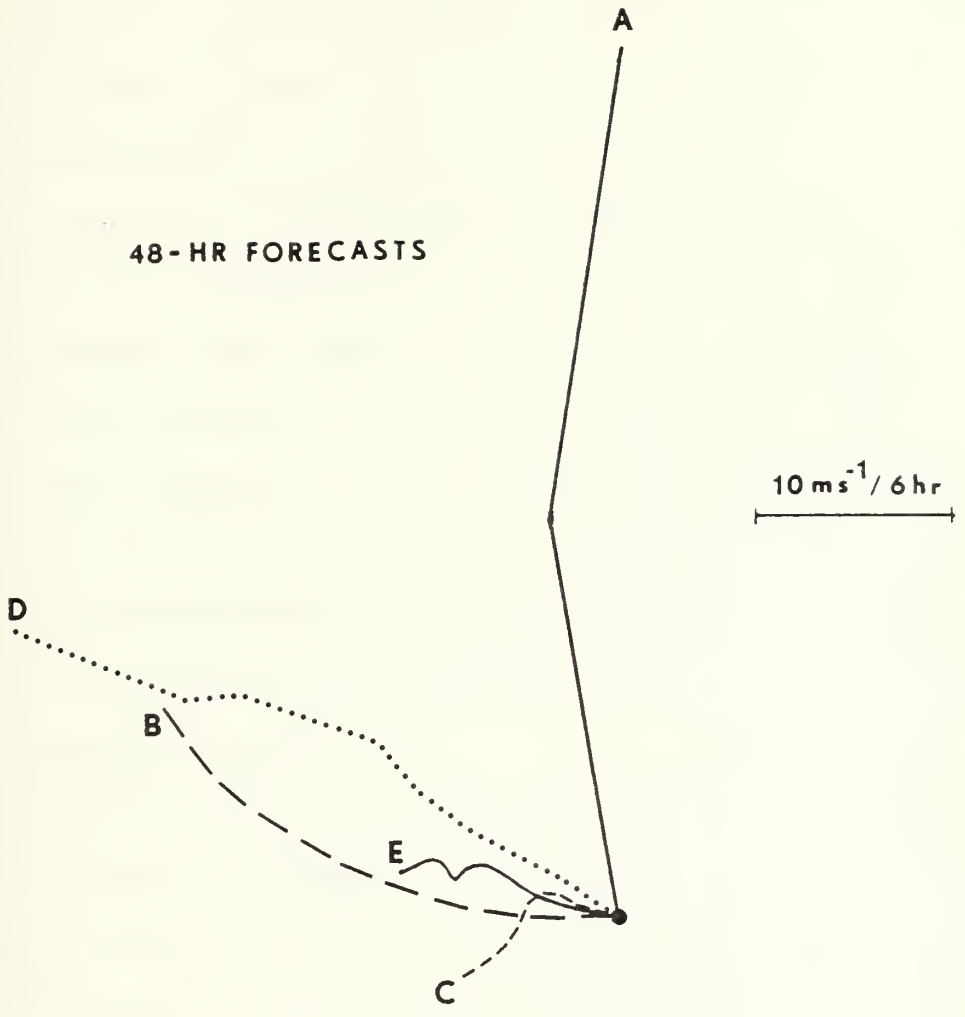

Fig. 17. Model forecast tracks from 00 GMT 04 Aug 1974 versus (A) best track and (B) unbiased and for a (C) Box-like, (D) Cosine and (E) basic bias function as in Fig. 15e.

bias correctors. The box-like biasing (C) resulted in an abnormal track forecast with an average speed of about one ms^{-1}. Although the cosine function (D) generally improved the forecast, increased weighting of the bias distorted seriously the cyclone wind fields. The forecast resulting from application of the basic biasing function (E) was not readily apparent as the optimum choice. However, upon increasing the weighting of the bias correctors, this was the only function which remained stable, even when applied with peak values an order of magnitude greater than the unit bias correctors. These corrections were easily tolerated by the TCM, since the solution for non-divergent wind components during reinitialization quickly reduced the added bias. That is, the wind fields needed to be over-adjusted to make the corrections effective.

The seven 1974 cases were used for testing the basic biasing function through differential component modifications. Analysis of track E (Fig. 17) suggests the need for a stronger northerly bias. The unit bias correctors for this case were $\Delta u = 0.8$ ms^{-1} and $\Delta v = 3.8$ ms^{-1}. Not as obvious was the need for less easterly bias since Δu seemed to have reduced the speed of track E. Therefore, to force greater northward movement while maintaining acceptable forecasts from all test cases, the Δv peak bias was increased as the Δu peak bias was decreased. The resulting biasing function for the v component is shown in Fig. 18. It was found for this limited sample that no u bias or negative v bias was necessary. The

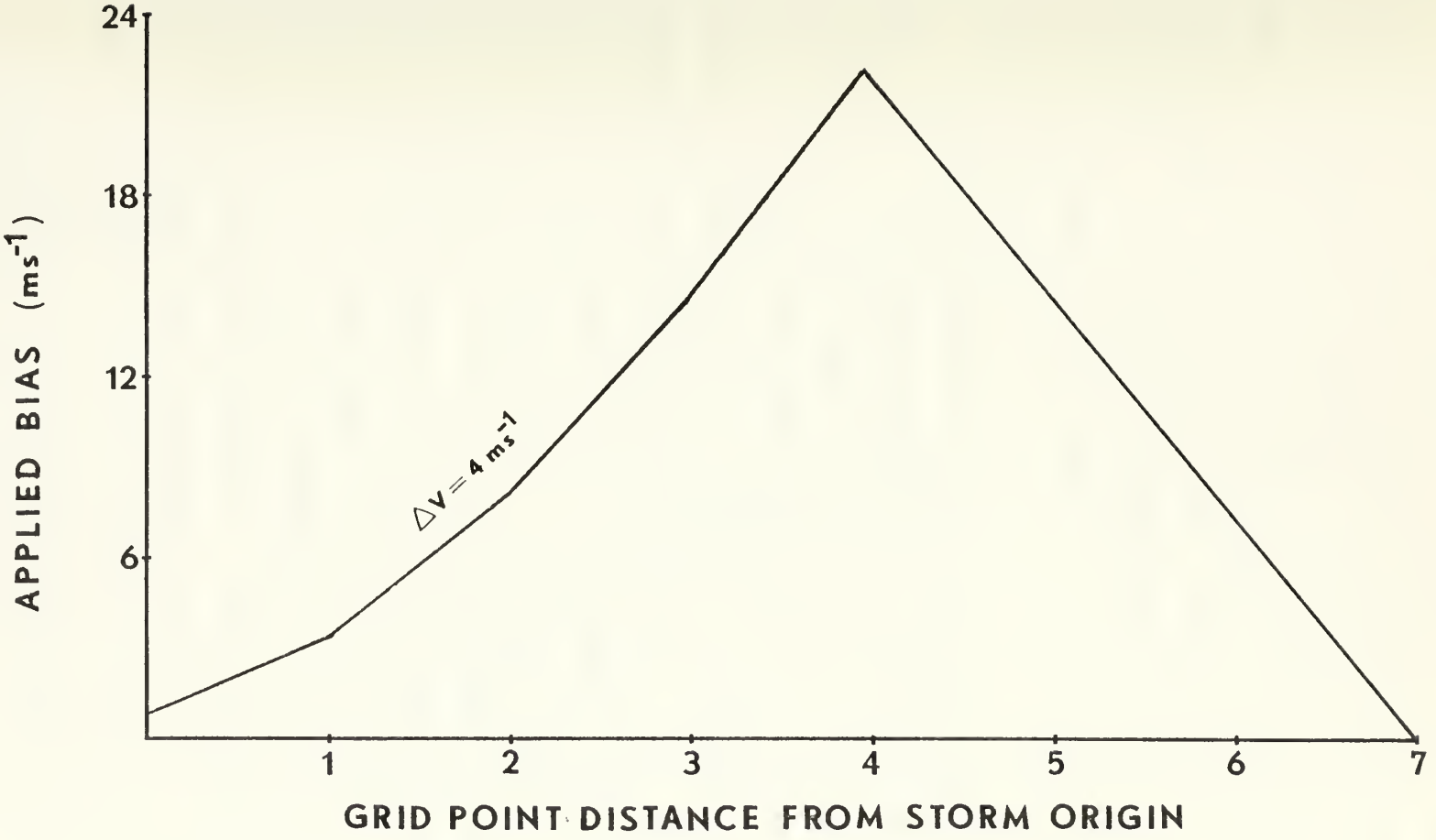

Fig. 18. Biasing function for a v-component bias corrector derived after differential adjustment tests with the 1974 cases.

general shape of this curve resembles the basic biasing function of Fig. 15e, but the slightly non-linear slope was found to produce better results. Because of the large v bias used, this was a successful effort to reduce distortion of the central vortex by the bias. As shown by Fig. 18, the v-component corrections for a Δv of 4 ms^{-1} would be extremely large. Even a bias corrector of 2 ms^{-1} would require a peak value of 6.5 ms^{-1}. It should be emphasized that the very large forcing of the v-component was peculiar to the small domain version of the TCM used.

The final results for all four Gilda cases are shown in Fig. 19. The actual storm path is plotted for the 0000 GMT positions. Note that the storm actually recurved while all of the unbiased forecast tracks were basically westward. Each biased forecast track is a result of biasing twice using weighting function represented in Fig. 15e. These biased forecasts resulted in little and moderate improvements for days 01 and 02 respectively. Excellent results were obtained for both days 03 and 04. The significant accomplishment of this biasing scheme was to make the storm recurve. The results for the other three cases (not plotted), for Typhoon Irma on 25, 26, and 27 November 1974, did not significantly alter the unbiased forecasts. The biased forecasts for Irma had an average error increase of only 37 km for the 48-hour period. Since the actual storm and unbiased tracks both moved westward, it was difficult to improve forecasts that were already very good (Ley, 1975).

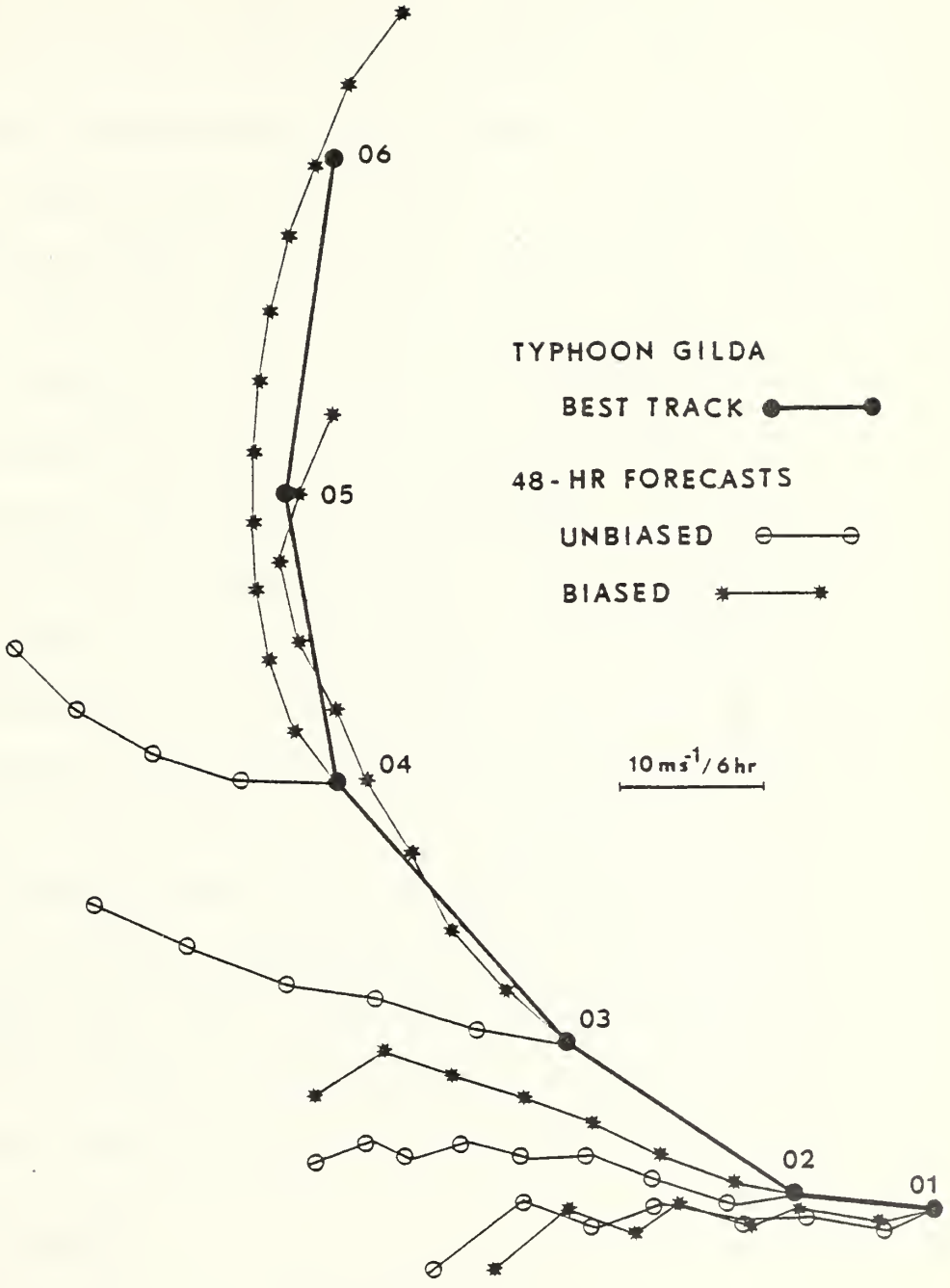

Fig. 19. Model forecasts with bias distribution as in Fig. 15e for the 01-04 Aug. 1974 cases.

Table I presents the forecast error averages for both this biasing method and the empirical approach based on George and Gray (1976) as described above. The number of biased forecasts which equalled or exceeded the unbiased forecasts are also tabulated for each six-hourly forecast interval. Figs. 20 and 21 depict graphically the averaged errors and standard deviations (respectively) from Table I. As originally required of this biasing scheme, the initial forecasts did improve. In fact, these cases resulted in track forecast error decreases of about 40% during the first 30 hours and about 25% at 48 hours. The method based on George and Gray (1976) decreased forecast errors by about 20% on the average. The official JTWC 24- and 48-hour forecast errors for the same seven forecast periods are also plotted in Fig. 20 for comparison. Not only did biasing by the first approach significantly decrease the TCM forecast errors, but also gained more accuracy over JTWC's official forecasts. Of equal significance, if not more so, are the standard deviation curves in Fig. 21. This graph shows that by biasing, especially by the first approach, there was less than half the variance of that resulting from the unbiased forecasts. The biasing resulted in tracks that were much more stable during the entire forecast period.

B. THE 1975 CASES

These 41 (originally) cases were initialized from the FNWC objectively-analyzed data (GBUA). All cases were used for calculation of the prediction equation regression coefficients. Of the original series, three cases were not

TABLE I

Method	Unbiased	First Bias		Second Bias	
Statistic	I	I	II	I	II
06 hr (7)	43	25	(5)	36	(4)
12 hr (7)	79	44	(6)	62	(4)
18 hr (7)	119	65	(5)	85	(5)
24 hr (7)	162	97	(5)	113	(4)
30 hr (7)	215	127	(5)	164	(5)
36 hr (7)	270	189	(5)	207	(5)
42 hr (7)	331	258	(5)	275	(5)
48 hr (7)	426	321	(5)	394	(4)

Mean 6-hourly forecast errors (km) (I) based on Best track for the 1974 cases for the unbiased, first bias and second bias approaches. The error at each 6-h interval is normalized by the initial position error. Also tabulated are the number of cases (II) which equal or exceed the unbiased error.

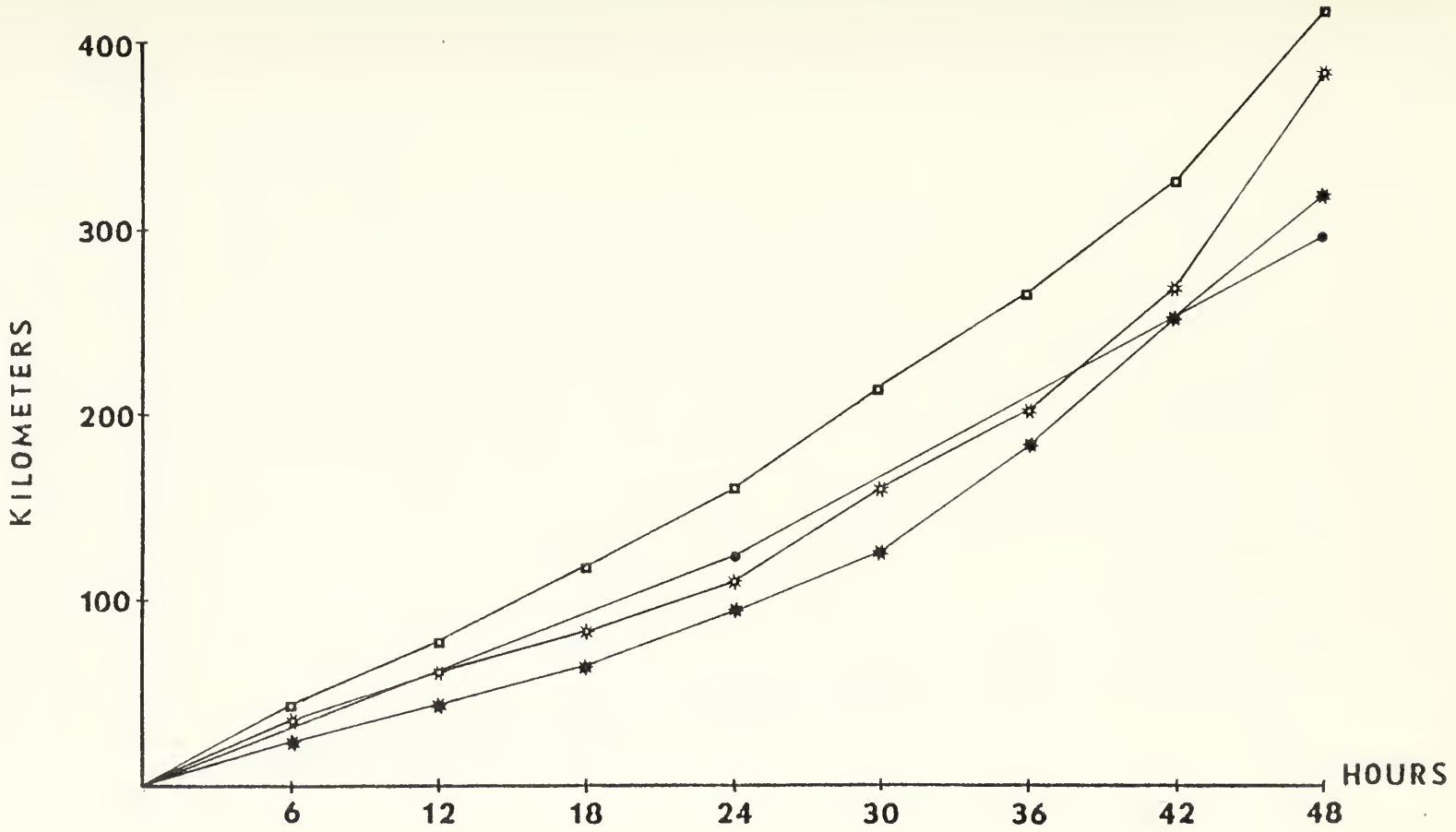

Fig. 20. Average forecast error (km) with 1974 cases for JTWC (•), unbiased model (▫), first bias (✱) and second bias (✱) techniques. The error at each 6-h interval is normalized by the initial position error.

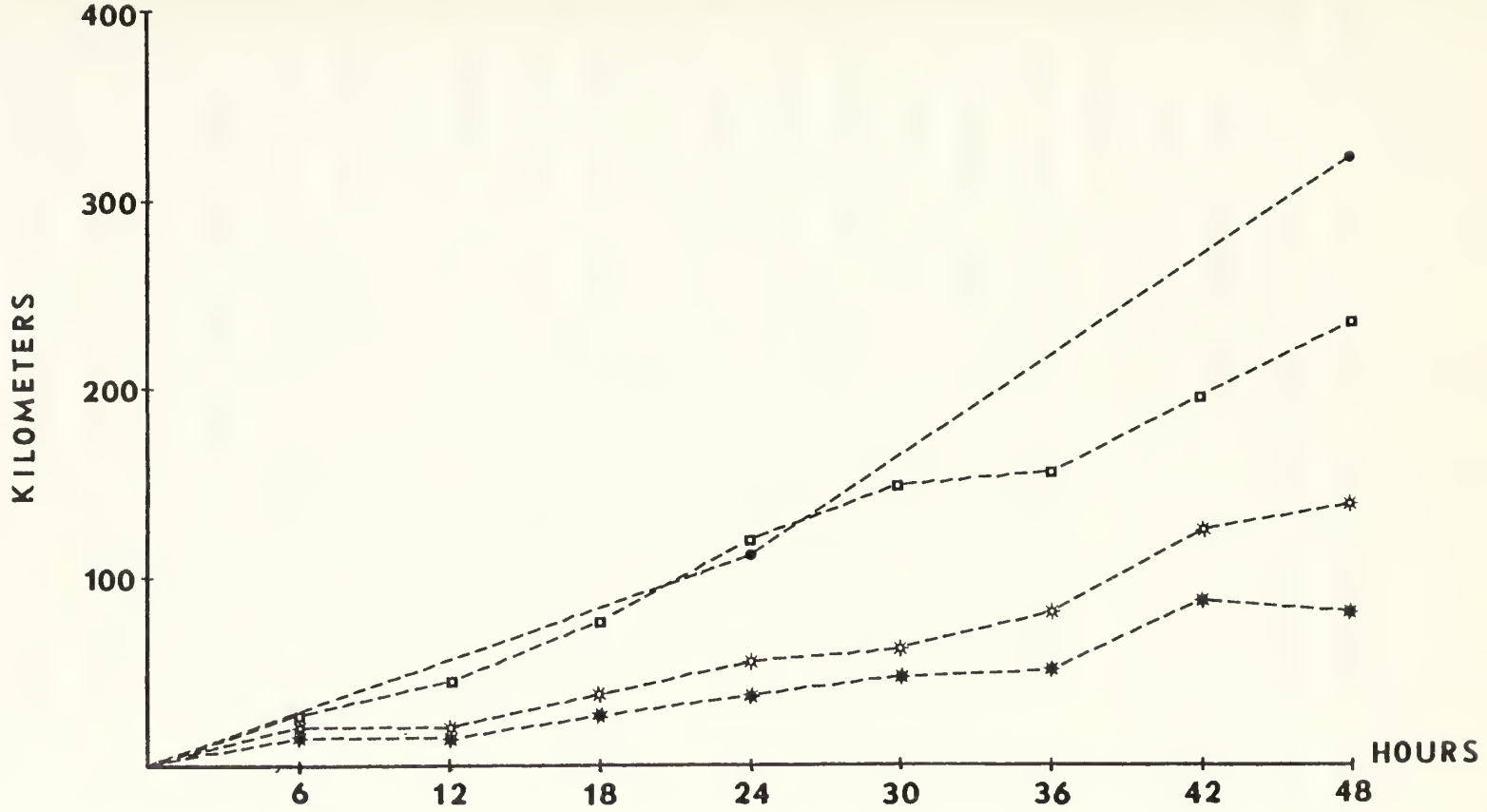

Fig. 21. Same as Fig. 20 except for standard deviation of track errors (km).

forecastable because the TCM's time step was not adjusted for storms occurring in the higher latitudes. Notable differences between the two series of tests (1974 and 1975) included the regression coefficients, the final forms of the biasing functions, the use of operational data versus hand-analyzed data, and model domain sizes. The results from an entire season of tropical storms should reveal how flexible this biasing scheme is.

The same basic biasing function from the 1974 cases (Fig. 15e) was used for obtaining the final biasing form best suited for the TCM version at FNWC. Again, differential biasing experiments were conducted by systematically adjusting the peak value of one bias corrector while holding the other fixed, and then vice versa. Because the FNWC TCM was four grid points wider and longer, a u-component bias was necessary, as had been expected. But after application of the resulting biasing function, the error showed less improvement than expected. In fact, the biasing increased the average forecast error, but only about 5%. Some of the error may be attributed to the estimate of the initial model storm movement, since the statistical regression equation based on the 1975 data only explained about 70% of the variances, as compared to 99% for the 1974 cases. However, the main source of error appears to be the initial data fields used by the TCM. First, several of the storms were not properly bogused. This was discovered by comparing the JTWC operational surface analyses with the initial 850-mb wind fields. These same

wind fields also revealed discrepancies within the original GBUA analyses (see Elsberry, 1977). Another possible cause was that several cases with maximum winds below 50 kts were included in the sample. The operational version of the TCM is only used for storms exceeding 50 kts. One might also note that the biasing scheme had little beneficial effect for the 01 August 1974 case in Fig. 19, when Gilda had 40 kt maximum winds. Analysis of the individual 1975 cases suggested that the biasing function would be more effective if the peak biasing value was proportional to storm intensity. However, in the form tested here, the biasing did not depend on storm intensity. During these tests, it was observed that a significant division of results from weak versus strong biasing occurred about the 60 kt maximum wind speed. Therefore, in an effort to test this biasing scheme on a more-or-less congruous sample, the only cases (24) tested were storms having maximum winds of 60 kts or greater and those with good initial analyses and vortex boguses. Since greater importance was placed on the more developed storms, the biasing function was adjusted to perform best with the stronger storms.

Having thus defined the test sample, differential bias testing produced the biasing function represented in Fig. 22. Although these curves show the bias that would be applied if both bias correctors, Δu and Δv, were 4 ms^{-1}, most of the bias correctors were about 1-5 ms^{-1}. The negative correction values are also shown. Note that the slopes are identical to that of the basic biasing function. This sample (linear)

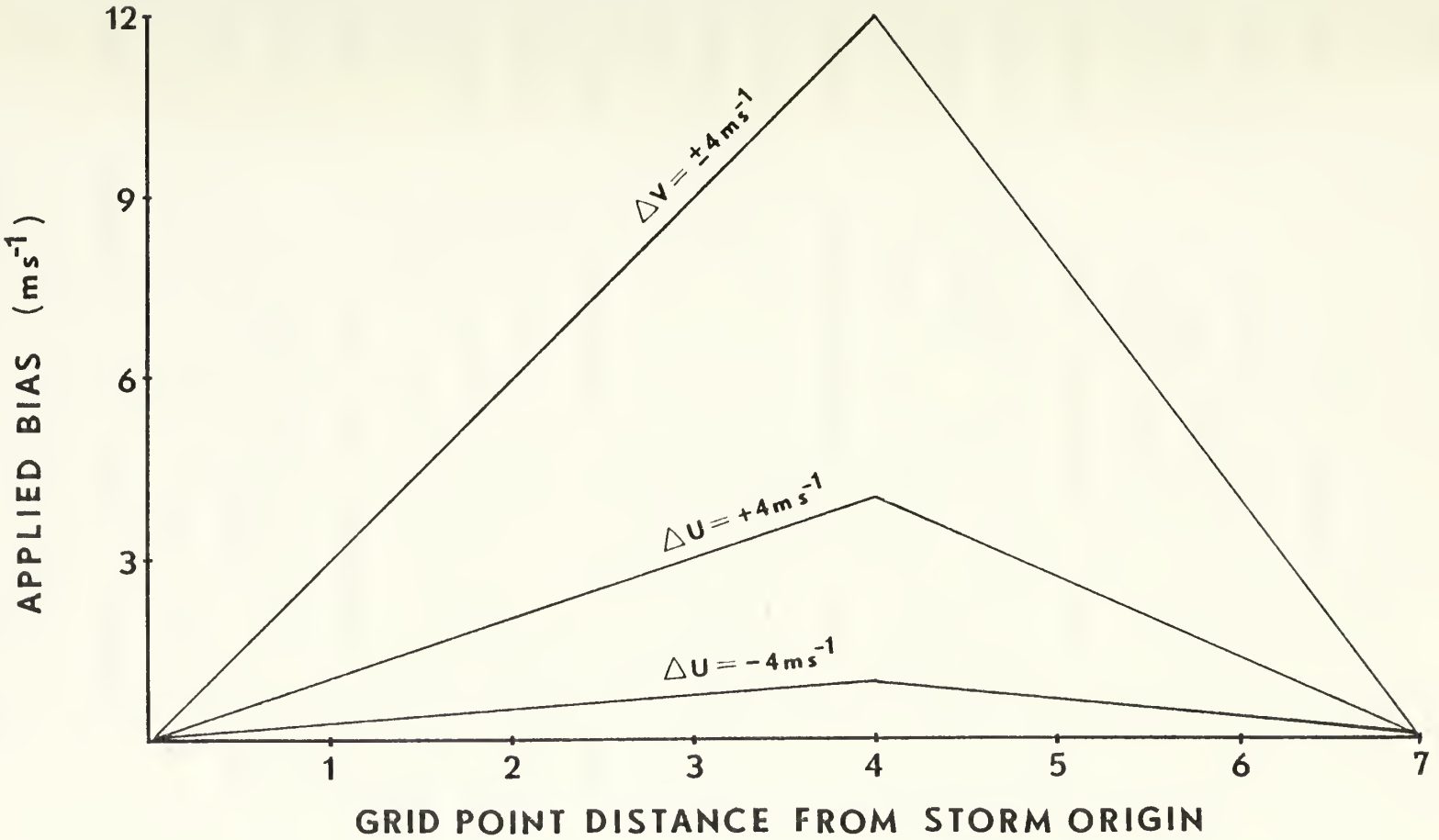

Fig. 22. Same as Fig. 18 except for 1975 cases, including the positive and negative zonal component correctors.

function was sufficient, since the large bias required for the 1974 cases (and resulting non-linear slope) was unnecessary due to the wider TCM channel. In general, only half as much v-component bias was required in this TCM as compared to that needed by the 1974 series TCM. The positive (eastward) and negative (westward) u-component corrections required for the same 4 ms^{-1} unit corrector are only one-third and one-twelfth the strength needed by an equivalent v-component unit corrector. These functions indicate that a combination of mostly northerly and some easterly bias will aid storm recurvature in the model. Fig. 23 illustrates graphically the respective weights of these differential corrections. The central x-y axes represent the unit bias corrector values, to be applied at the fourth grid square as in Fig. 22. By imagining Fig. 23 relative to a channeled TCM, one can visualize the greater bias applied by v-component and positive u-component correctors. Note that the peak u biasing scales are four times smaller than the v biasing scale. The negative v-component was biased just as heavily as the positive component. It was also observed that large biasing by one component relative to the other component often resulted in poorer forecasts. This was especially true if this other component was less than 1 ms^{-1}. Therefore, the dashed lines determine a component's peak value under conditions determined by the other component's unit value. In general, if Δu was less than $\frac{1}{2}$ ms^{-1}, then the peak v value would be reduced by 75%. If the absolute value of Δv was less than 1 ms^{-1}, then the peak u value would also be reduced by 75%.

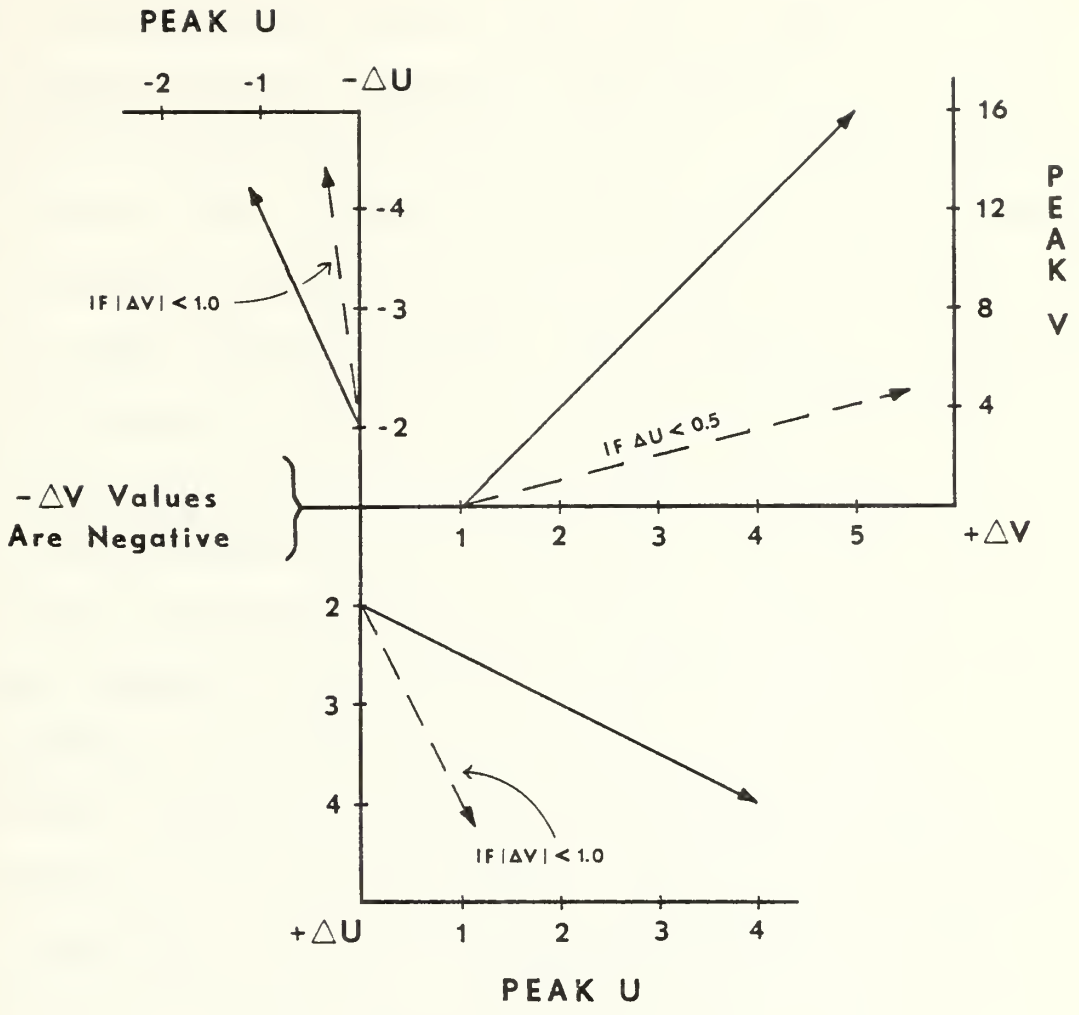

Fig. 23. Peak biasing values for the 1975 cases as a function of direction and magnitude of the bias correctors (ms^{-1}).

The error statistics resulting from the 1975 test cases are presented in Table II. The unbiased and biased TCM and the JTWC 48-hour forecast errors are shown in Fig. 24. The biasing scheme attained consistent improvements over the unbiased cases throughout the forecast period. Forecast errors with the biased model versus the unbiased model were decreased about 30% during the first 30 hours and about 15% after 48 hours. The JTWC official forecasts were equalled or exceeded by the TCM forecasts with biasing. Average standard deviations for the unbiased and biased forecasts are shown in Fig. 25. The biasing decreased storm track variations by about 45% for the first 36 hours. As with the 1974 case results, the decrease of the standard deviation error was the most significant achievement of biasing.

The above comparison of biased and unbiased forecasts was in terms of the relative errors. That is, the positional errors originating during initialization were not included. A comparison of the same forecast schemes as in Fig. 24, with the inclusion of the errors due to the poor initial bogus of the storm location, is shown in Fig. 26. Even with this crude model, the bias adjustments produced results after 30 hours nearly equivalent to JTWC official forecasts. Including the 41 unbiased cases, the average initial position error for the TCM was 85 km, whereas the official JTWC position error was only 34 km. Therefore, the effects of biasing cannot be expected to improve this error, since the biasing procedures are based on the wind fields provided by

TABLE II

Method	Unbiased	First Bias	
Statistic	I	I	II
06 hr (23)	81	55	(21)
12 hr (23)	128	69	(21)
18 hr (23)	182	125	(22)
24 hr (22)	232	171	(17)
30 hr (18)	289	214	(13)
36 hr (17)	345	267	(13)
42 hr (13)	349	311	(8)
48 hr (13)	413	363	(10)

Same as Table I except for the 1975 cases and without the second bias method.

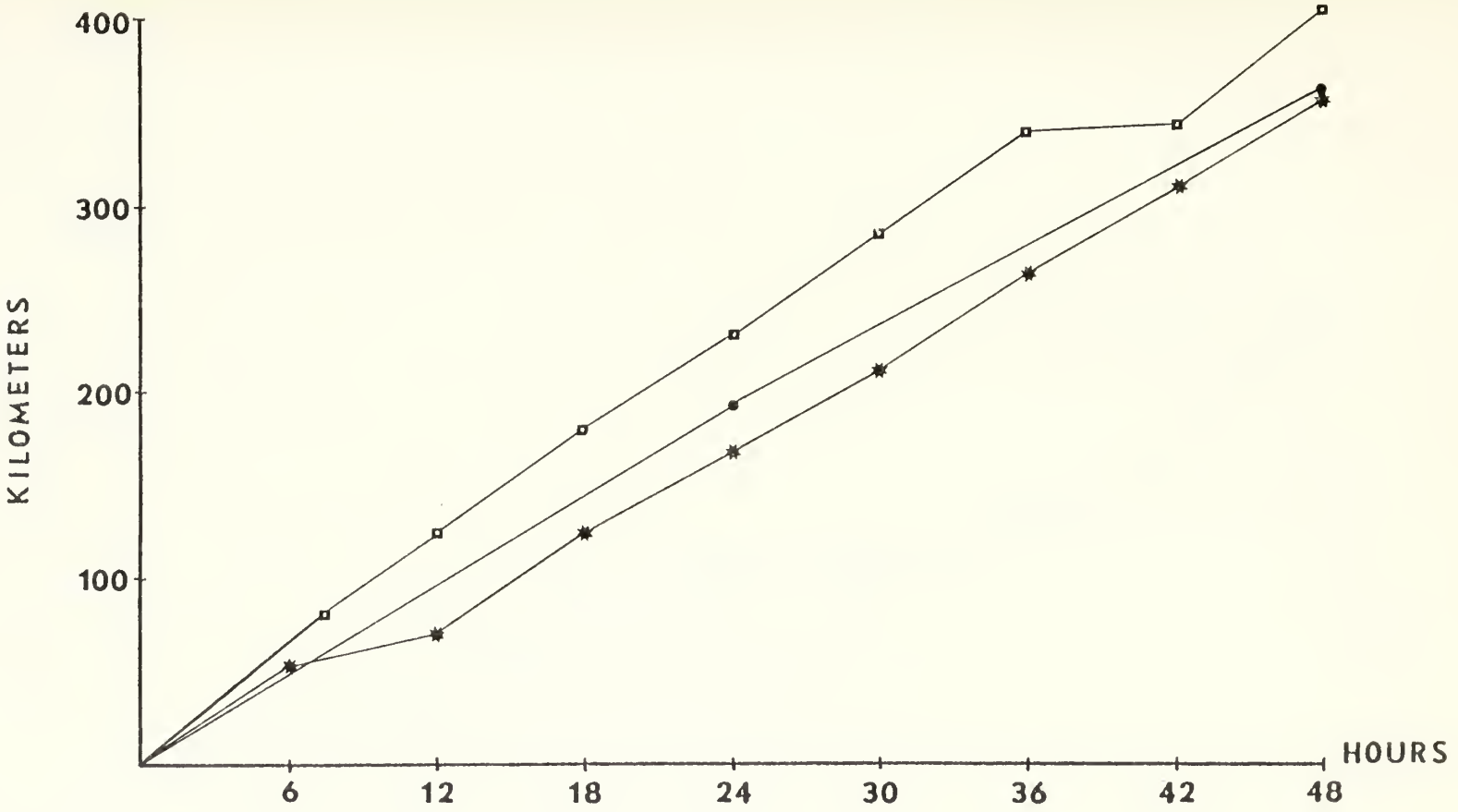

Fig. 24. Same as Fig. 20 except for 1975 cases.

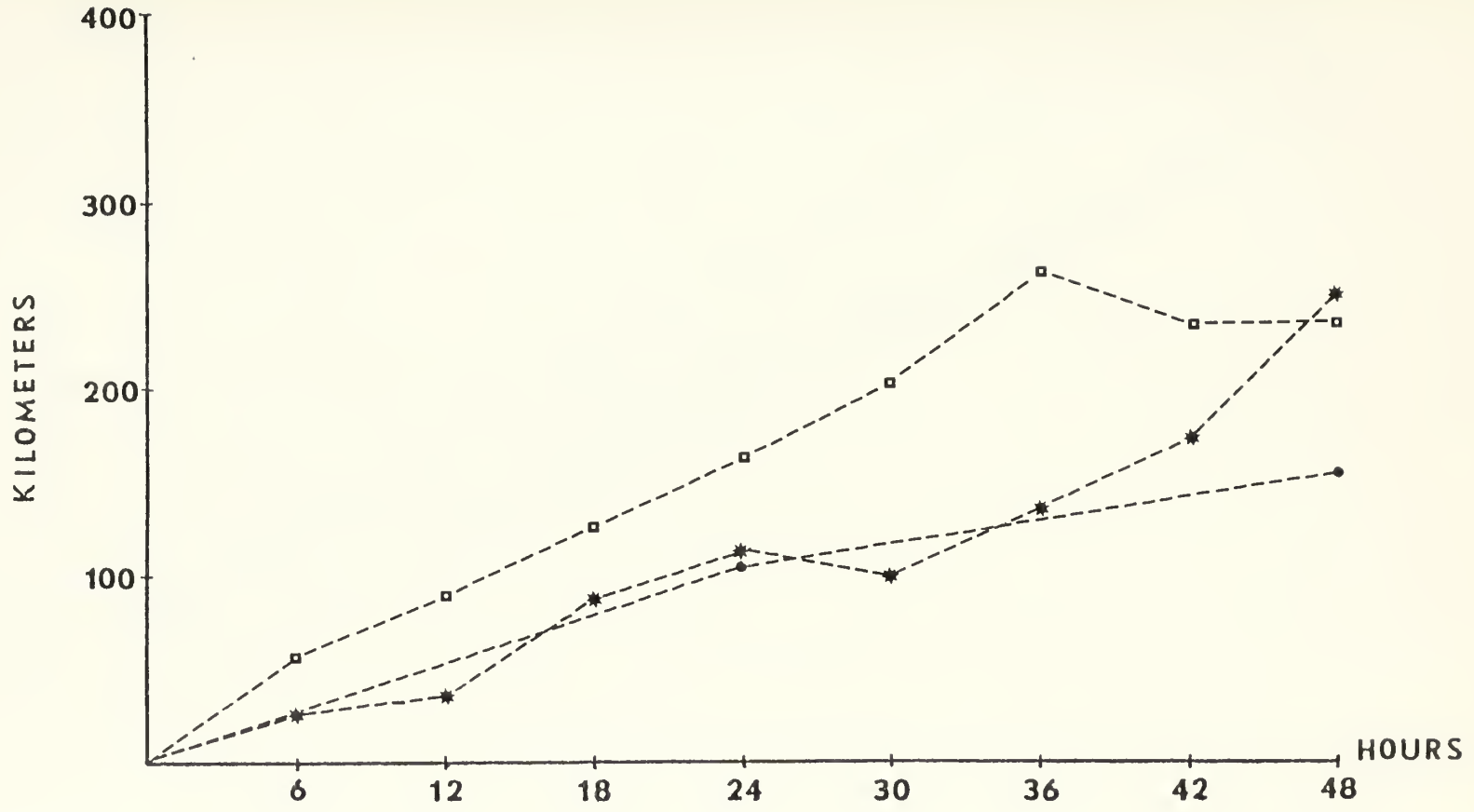

Fig. 25. Same as Fig. 21 except for 1975 cases.

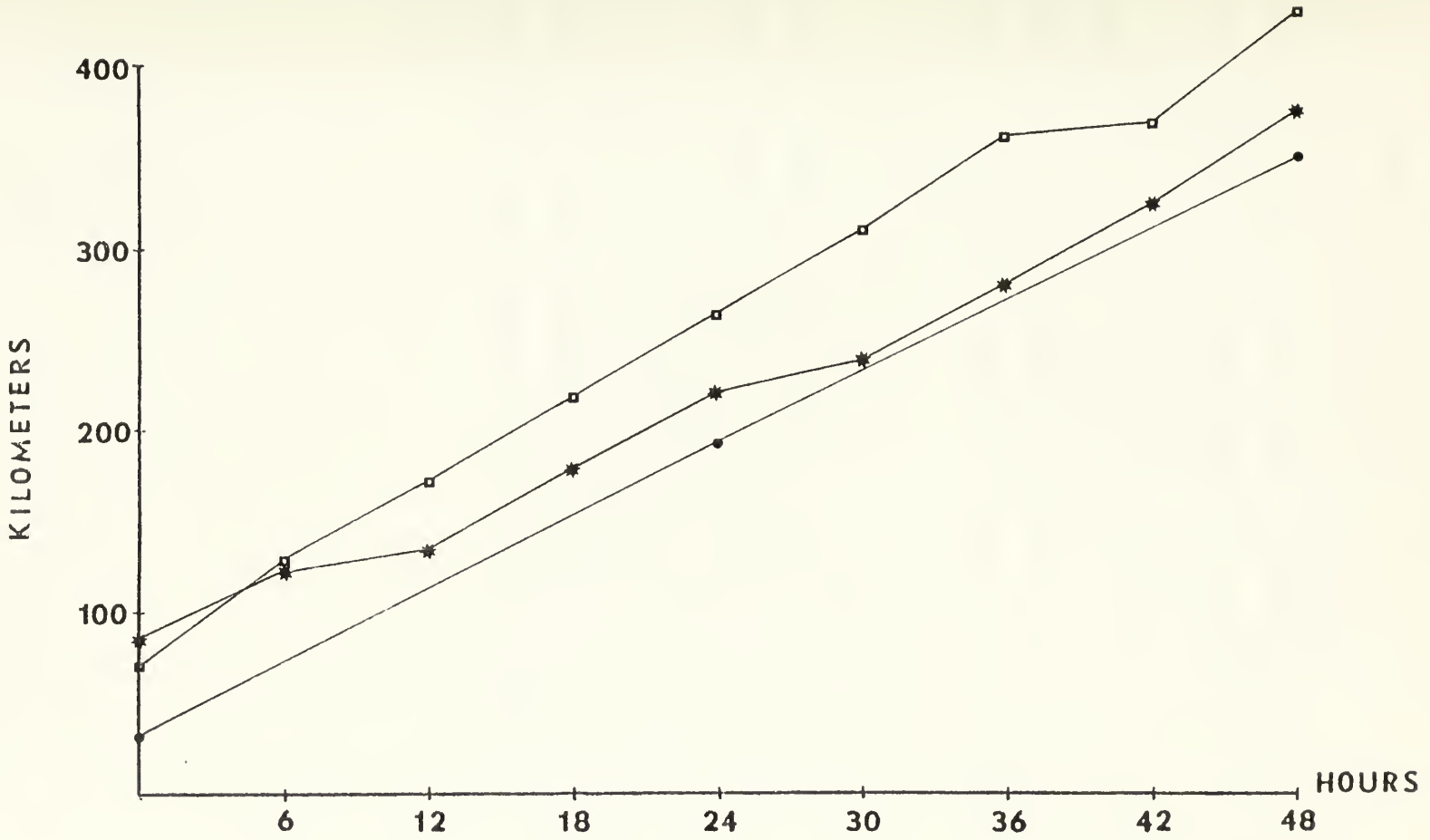

Fig. 26. Same as Fig. 24 without normalization by initial position error.

the initial storm bogusing. But it should be noted that the biasing scheme did introduce an additional initial error of about 15 km. As a result of determining the average steering current and applying the bias corrections based on the grid point nearest the storm center, the adjusted steering current may have become asymmetrical. Adding too much bias in one quadrant evidently alters the storm circulation center. This problem should be solved by using interpolation schemes for both the steering current averages and the application of bias corrections.

Of the 24 test cases, two of the forecasts with the bias did not complete the 48-hour period. One case could not be tracked after 24 hours. No apparent explanation was found, but the bias may have adversely affected the vortex structure. The second case was comparatively weak (70 kts), which suggests that an intensity-proportional biasing function may have reduced the bias applied and possibly permitted a 48-hour forecast.

VI. CONCLUSIONS

A primitive-equation tropical cyclone forecast model (Ley and Elsberry, 1976) is being tested at FNWC (Hinsman, 1977) with operational data. The objective of this research was to improve the initial model storm tracks by incorporating the observations of actual storm motion that would be available before the model is run. Development consisted of testing two series of initialization data. The 1974 data cases were hand-analyzed by JTWC, while the 1975 data cases were objectively analyzed by FNWC. Two biasing approaches were developed. The first was based on a statistical regression prediction of initial storm motion while the second used an empirical relationship (see George and Gray, 1976) to define the steering current.

The largest improvements occurred within the 12- to 36-h periods, and the effects continued beyond 48 h. This result was found with both the 1974 and 1975 cases. The relatively large errors for the first 6-h forecasts during 1975 can be attributed to two effects. First, most dynamical models require an adjustment period of 6 to 12 hours. Second, it requires some time for the effect of the bias adjustments at relatively large distances from the storm center to take effect. Some attempts were made to apply enough bias to make the initial 6-h forecast nearly parallel to the desired track. However, such extreme biasing always resulted in an

abnormal track during later periods because excessive biasing of the initial wind fields resulted in severe deformation of the synoptic features.

It should be pointed out that the weakest link in this biasing scheme is the prediction of the initial storm motion. The regression coefficients have not been tested with an independent sample of storms. Application of the statistical equations in the future may not produce comparable results. Even the estimation of the steering current based on George and Gray (1976) is based on historical correlations and may not be relevant during an abnormal storm season, such as during 1975. A superior approach would be to run the model for six hours, which can then be compared to the actual storm motion. This procedure would require some additional computer resources but would eliminate the uncertainty associated with the statistical regression equation. These regression coefficients may also be geographically dependent and thus may be limited to the western Pacific region. Elimination of the prediction equation would therefore permit application of this biasing scheme to other regions.

A major source of error encountered with the 1975 test cases was the quality of the data fields originally supplied to the model (see Elsberry, 1977). The objectively-analyzed wind fields (GBUA) were significantly inferior to the hand-analyzed cases. The storm bogus, which initially positions and defines the vortex, not only misplaced the storm center, but the intensity and vertical structure were unrealistic at

times. Further attempts to improve this biasing scheme should not be attempted until the bogusing routine is improved.

This thesis found an effective method for applying the bias horizontally, but there is still some uncertainty as to how to apply the bias in the vertical. It is expected that a vertically dependent biasing scheme will produce better results. This should be especially applicable to the 250-mb level where cyclonic outflow patterns may need special treatment. It is also suggested that a simple intensity-proportional biasing function should produce better results, because storms with less than 60 kts were more sensitive to strong bias corrections.

This biasing scheme can improve the dynamical model forecast accuracy by using the actual storm motion, which is currently available when the operational model is begun. The potential abilities of this method were observed with the 1974 series results. Operational use is presently possible if the most recent storm track is well known. Elimination of the prediction equation and the inclusion of a storm intensity-weighting biasing function should lead to improved forecast guidance from the dynamical model.

APPENDIX: THE TROPICAL CYCLONE MODEL

A. THE MODEL

The primitive equation model developed by Elsberry and Harrison (1971) and Harrison (1973) was used as the basis for these experiments. Although this model is capable of triply-nested operation, insufficient time limited testing to the uniform, coarse-mesh grid version. The model equations are:

$$\frac{\partial u}{\partial t} = -L(u) + fv - M\frac{\partial \phi}{\partial x} + \frac{\partial \tau_{xx}}{\partial x} + \frac{\partial \tau_{yx}}{\partial y} \qquad \text{(A-1)}$$

$$\frac{\partial v}{\partial t} = -L(v) - fu - M\frac{\partial \phi}{\partial y} \quad \frac{\partial \tau_{xy}}{\partial x} + \frac{\partial \tau_{yy}}{\partial y} \qquad \text{(A-2)}$$

$$\frac{\partial \theta}{\partial t} = -L(\theta) \qquad \text{(A-3)}$$

$$\frac{\partial \phi_{1000}}{\partial t} = -L(\phi_{1000}) \qquad \text{(A-4)}$$

$$\frac{\partial \omega}{\partial p} = -M^2\left[\frac{\partial}{\partial x}\left(\frac{u}{M}\right) + \frac{\partial}{\partial y}\left(\frac{v}{M}\right)\right] \qquad \text{(A-5)}$$

$$\frac{\partial \phi}{\partial p} = \theta\, C_p \frac{\partial}{\partial p}\left(\frac{p}{1000}\right)^{R/C_p} \qquad \text{(A-6)}$$

where

$$L(S) = M^2\left[\frac{\partial}{\partial x}\left(\frac{us}{M}\right) + \frac{\partial}{\partial y}\left(\frac{vs}{M}\right)\right] + \frac{\partial}{\partial p}(\omega s)$$

L(S) represents the flux divergence of any scalar quantity S. The other meteorological symbols used above can be found in the "List of Symbols".

The linear computational stability criterion for two-dimensional equations governing simple wave motion is

$$\frac{C\Delta t}{\Delta x} \leq .707 \qquad \text{(A-7)}$$

where

$C \equiv$ the phase velocity of the fastest gravity wave

$\Delta t \equiv$ time increment

$\Delta x \equiv$ horizontal grid increment

Eq. (A-7) dictates a maximum time step of 480 seconds for this model. An increase to 800 seconds was achieved by time averaging the pressure gradient term of the momentum equations (see Ley, 1975). The 800-second time step was used for testing the 1974 cases, while a 600-second time step was used for testing the 1975 cases as the relocatable grid was extended northward where Δx is reduced.

The initial step was forward in time. All subsequent iterations used the leap-frog scheme. Parameterization of latent heat release was not possible because moisture fields were not available. Consequently, friction was also neglected, so that the TCM forecasts storm movement primarily by advective processes.

B. THE GRID

The uniform, coarse-mesh grid is a mercator projection true at 22.5°N. The horizintal grid increment was nominally 220 km. The grid extended 28 grid points east-west and 20

grid points north-south for the 1974 cases. An extra four grid points east-west and north-south were used for the 1975 cases. The grid was oriented such that each storm was initially centered near the 17th column and the 10th row to allow for movement into the NW quadrant. Fig. A-1 shows the vertical distribution of dependent parameters. Although the variables are staggered in the vertical, horizontal space staggering was not utilized in these experiments.

C. BOUNDARY CONDITIONS

Boundary conditions on the northern and southern walls were the no-flux type after Elsberry and Harrison (1971). These conditions are

$$\phi_{j+1} = \phi_j \tag{A-8a}$$

$$v_{j+1} = -\frac{M_{j+1}}{M_j} v_j \tag{A-8b}$$

$$u_{j+1} = u_j \tag{A-8c}$$

Such a representation actually places the wall between the outer two grid rows on the poleward and equatorial sides. Mass is conserved along these boundaries since the v component is always zero at the wall; in essence, the wall is a streamline. Thus, the 18 grid rows of extracted data were expanded to 20 rows with the inclusion of the no-flux boundaries.

The east-west boundaries were made cyclic after Krishnamurti (1969). This procedure, applicable to the

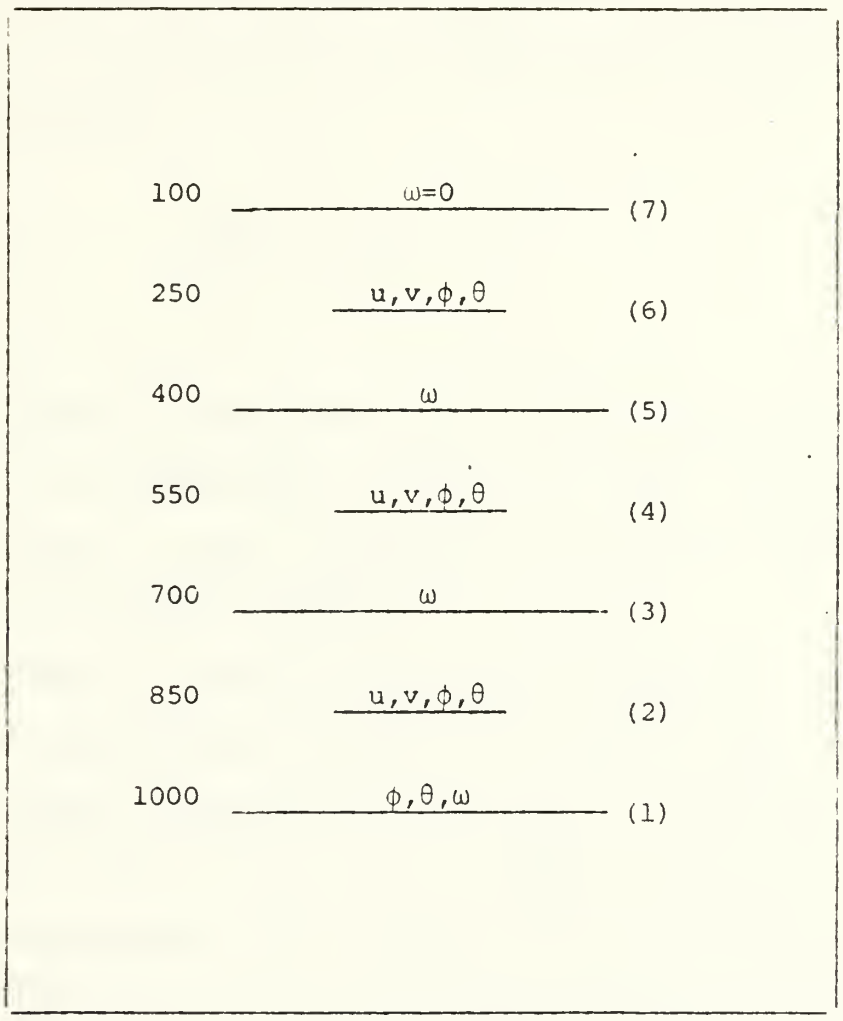

Fig. A-1. Vertical distribution of dependent variables and pressure levels for the three-dimensional model (after Harrison, 1973).

1000-mb height field and the 850-, 500-, and 250-mb u and v fields, adds a buffer zone in the east-west direction to absorb the impact of forced continuity. For the 1974 cases, the original data of 23 longitudinal columns was expanded to 28 columns by adding one column to the west side and four columns to the east side. The values in this buffer zone were determined by

$$S_{28,j} = S_{2,j} \tag{A-9a}$$

$$S_{1,j} = S_{27,j} \tag{A-9b}$$

and then linearly interpolated to fill values in columns 25 through 27. The grid used for the 1975 cases was expanded in a similar manner. Here S represents any of the original data fields mentioned earlier.

The vertical velocity at the upper boundary is equal to zero and is calculated at levels 5, 3, and 1, Fig. A-1, through downward integration of Eq. (A-5). Optimum results were obtained when, in Eq. (A-4), $\omega \frac{\partial \phi}{\partial p}$ was replaced by the equivalent expression $-\omega\alpha$. Further solution improvement was attained when ω in Eq. (A-4) was represented by an averaged value from

$$\omega_{ij} = (\omega_{i,j+1} + \omega_{i,j-1} + \omega_{i+1,j} + \omega_{i-1,j} + 4\omega_{i,j})/8 \tag{A-10}$$

D. FNWC'S TROPICAL CYCLONE MODEL

The 1975 storms were run on a semi-operational basis using FNWC's TCM. This model was modified by R. Perry of the

Naval Environmental Prediction Research Facility (NEPRF) and Lt. D. Hinsman, USN, of FNWC to run with operational data. It has two significant improvements over the version used to forecast the 1974 storms. The model incorporates Robert time filtering and a direct solver instead of successive over-relaxation (SOR) (see Rosmond and Faulkner, 1976) to solve the Poisson equations for the initialization process. This model is currently supporting JTWC on an operational basis (Hinsman, 1977).

E. DIAGNOSTIC PHASE

The relative vorticity fields were obtained from the observed u and v components

$$\zeta_r = M^2 [\frac{\partial}{\partial x} (\frac{v}{M}) - \frac{\partial}{\partial y} (\frac{u}{M})] \qquad \text{(A-11)}$$

Subsequently the streamfunction, ψ, was found by sequential over-relaxation of the expression

$$\nabla^2 \psi = \zeta_r \qquad \text{(A-12)}$$

and the non-divergent wind components were calculated through

$$u_\psi = -M \frac{\partial \psi}{\partial y} \ , \ v_\psi = M \frac{\partial \psi}{\partial x} \qquad \text{(A-13)}$$

Solution of Eq. (A-12) requires specification of boundary values on the northern and southern peripheries. To remain consistent with the no-flux boundaries, described by Eqs. (A-8b and A-8c), constant streamfunction values were defined

for the northernmost and southernmost two rows. Following Elsberry and Harrison (1971), zero was chosen for the southern rows, and the northern values were calculated from

$$\tilde{\psi}_{north} = \tilde{\psi}_{south} - (\frac{\bar{u}_\psi}{M})\ \Delta y \qquad \text{(A-14)}$$

Here $\bar{u}_\psi$ is the mean zonal wind component averaged over the entire grid and Δy is the distance between the north and south walls.

An appropriate balance equation can be derived through partial differentiation of Eq. (A-1) with respect to x and Eq. (A-2) with respect to y. Addition of these two equations, plus rearrangement of terms, leads to

$$\frac{\partial}{\partial t}(M^2[\frac{\partial}{\partial x}(\frac{u_\psi}{M})+\frac{\partial}{\partial y}(\frac{v_\psi}{M})]) = -M^2[\frac{\partial}{\partial x}\frac{L(u_\psi)}{M}]-M^2[\frac{\partial}{\partial y}\frac{L(v_\psi)}{M}]+fM^2[\frac{\partial}{\partial x}(\frac{v_\psi}{M})-\frac{\partial}{\partial y}(\frac{u_\psi}{M})]$$

$$-M^2u_\psi\frac{\partial}{\partial y}(\frac{f}{M})-M^2[\frac{\partial^2\phi}{\partial x^2}+\frac{\partial^2\phi}{\partial y^2}] \qquad \text{(A-15)}$$

To begin the prognostic stage smoothly, the left hand side of Eq. (A-15) is set equal to zero. Surface diffusive effects were neglected. Manipulation of Eq. (A-15) leads to a Poisson equation,

$$\nabla^2\phi = -\frac{\partial}{\partial x}[\frac{L(u_\psi)}{M}]-\frac{\partial}{\partial y}[\frac{L(v_\psi)}{M}]+f[\frac{\partial}{\partial x}(\frac{v_\psi}{M})-\frac{\partial}{\partial y}(\frac{u_\psi}{M})]-u_\psi\frac{\partial}{\partial y}(\frac{f}{M})$$

(A-16)

that is readily solved with sequential over-relaxation or other direct methods. In this case, the mean geopotential value on the south wall was derived hydrostatically (Eq.

(A-6)) based upon a mean climatological temperature sounding. An average geopotential value for the north wall was found through integration of the v momentum equation (noting that $\frac{\partial v}{\partial t} = 0$) over the region.

$$\tilde{\phi}_N = \tilde{\phi}_S - [\bar{f} \cdot (\frac{\bar{u}_\psi}{M}) + \frac{\overline{L(v_\psi)}}{M}] \Delta y \qquad \text{(A-17)}$$

Again, Δy is the north-south grid distance. To assure maintenance of the no-flux boundary conditions, Eq. (A-8a) was now applied at all levels. Having found the balanced geopotential fields from the upper level wind fields, only the 1000-mb geopotential field and the temperature fields at levels 1, 2, 4, and 6, Fig. A-1, need to be specified to begin the prognostic phase. Since the initial wind fields are non-divergent, the vertical velocity is everywhere zero.

The 1000-mb geopotential field was obtained hydrostatically from the 850-mb values. This requires that the 1000-mb and 850-mb potential temperature fields are defined. From Eq. (A-6), recall that the thickness between two levels in the atmosphere is proportional to the mean potential temperature of the layer. Constant potential temperatures for the 1000-mb north and south walls were obtained from climatology. A linear gradient at 1000 mb was forced to fit the boundary values. It was assumed that the 850-mb potential temperatures were everywhere $4^{\circ}K$ warmer than the corresponding 1000-mb values. This assumption resulted in a linear meridional gradient in the 1000/850-mb layer mean potential temperature

field. Finally, the 1000-mb geopotential field and the 500-mb and 250-mb potential temperature distributions were obtained using Eq. (A-6).

LIST OF REFERENCES

Annual Typhoon Report, 1974-75: Fleet Weather Central/Joint Typhoon Warning Center, Guam.

Anthes, R. A., 1974: Data assimilation and initialization of hurricane prediction models. J. Atmos. Sci., 31, 702-719.

Elsberry, R. L., 1975: Feasibility of an operational tropical cyclone prediction model for the western North Pacific area. Tech. Report NPS-51Es75051, Naval Postgraduate School, 56 pp.

Elsberry, R. L., 1977: Operational data tests with a tropical cyclone model. Tech. Report NPS-63Es77031, Naval Postgraduate School, 28 pp.

Elsberry, R. L. and E. J. Harrison, Jr., 1971: Height and kinetic energy oscillations in a limited region prediction model. Mon. Wea. Rev., 99, 883-888.

George J. E. and W. M. Gray, 1976: Tropical cyclone motion and surrounding parameter relationships. J. Applied Meteo., 15, 1252-1264.

Haltiner, G. J., 1971: Numerical Weather Prediction, Wiley, New York, 317 pp.

Harrison, E. J., Jr., 1973: Three-dimensional numerical simulations of tropical systems utilizing nested finite grids. J. Atmos. Sci., 30, 1528-1543.

Hinsman, D. E., Lt. USN, 1977: Preliminary results from the Fleet Numerical Weather Central tropical cyclone model. Third Conference on Numerical Weather Prediction, AMS, Omaha, Nebr.

Hovermale, J. B., H. S. Scolnik and D. G. Marks, 1976: Performance characteristics of the NMC movable fine mesh model (MFM) pertaining to hurricane predictions during the 1976 hurricane season. Unpublished report, NMC.

Krishnamurti, T. N., 1969: An experiment in numerical prediction in equatorial latitudes. Quart. J. Roy. Meteor. Soc., 95, 594-620.

Ley, G. W., 1975: Some design experiments for a nested grid forecast model of western Pacific tropical cyclones, M.S. Thesis, Naval Postgraduate School, Monterey, California.

Ley, G. W. and R. L. Elsberry, 1976: Forecasts of Typhoon Irma using a nested-grid model. Mon. Wea. Rev., 104, 1154-1161.

Pike, A. C., 1972: Improved barotropic hurricane track prediction by adjustment of the initial wind field. NOAA Technical Memo NWS SR-66.

Renard, R. J., S. G. Colgan, M. J. Daley and S. K. Rinard, 1972: Numerical-statistical forecasts of tropical-cyclone tracks by the MOHATT scheme with application to the north Atlantic area. Tech. Note No. 72-4, Naval Postgraduate School, Monterey, California.

INITIAL DISTRIBUTION LIST

		No. Copies
1.	Defense Documentation Center Cameron Station Alexandria, Virginia 22314	2
2.	Library, Code 0142 Naval Postgraduate School Monterey, California 93940	2
3.	Dr. G. J. Haltiner, Code 63Ha Department of Meteorology Naval Postgraduate School Monterey, California 93940	1
4.	Dr. R. L. Elsberry, Code 63Es Department of Meteorology Naval Postgraduate School Monterey, California 93940	7
5.	Captain John D. Shewchuk Det 1, 1WWg COMNAVMAR Box 17 FPO San Francisco 96630	5
6.	Commanding Officer Fleet Numerical Weather Central Naval Postgraduate School Monterey, California 93940	1
7.	Department of Meteorology, Code 63 Naval Postgraduate School Monterey, California 93940	1
8.	Commanding Officer Naval Environmental Prediction Research Facility Naval Postgraduate School Monterey, California 93940	1
9.	Air Weather Service (AWVAS/FT) Scott AFB, Illinois 62225	1
10.	Mr. S. Brand Naval Environmental Prediction Research Facility Naval Postgraduate School Monterey, California 93940	1

11. Dr. S. Burk — 1
Naval Environmental Prediction Research Facility
Naval Postgraduate School
Monterey, California 93940

12. Dr. C. P. Chang, Code 63Cj — 1
Department of Meteorology
Naval Postgraduate School
Monterey, California 93940

13. Commanding Officer — 2
Fleet Weather Central/Joint Typhoon Warning Center
COMNAVMARIANAS Box 12
FPO San Francisco 96630

14. Lieutenant Donald E. Hinsman — 1
Fleet Numerical Weather Central
Monterey, California 93940

15. Mr. R. Hodur — 1
Naval Environmental Prediction Research Facility
Naval Postgraduate School
Monterey, California 93940

16. Captain Harry Hughes — 1
AFIT/CIPF
Wright-Patterson AFB, Ohio 45433

17. Director, Naval Oceanography and Meteorology — 1
National Space Technology Laboratory
Bay St. Louis, Mississippi 39520

18. Dr. T. Rosmond — 1
Naval Environmental Prediction Research Facility
Naval Postgraduate School
Monterey, California 93940

19. Commander F. R. Williams, Code 63Wf — 1
Department of Meteorology
Naval Postgraduate School
Monterey, California 93940

Thesis
S4625
c.1

Shewchuk
Development of a biasing scheme to improve initial dynamical model forecasts of tropical cyclone motion.

171822